WL-TR-91-2019

NEGATIVE ION FORMATION WITH ELECTRON IMPACT TO SIMULANTS

P. G. Datskos, L. A. Pinaduwage, L. G. Christophorou, and J. G. Carter

Oak Ridge National laboratory
Oak Ridge, Tennessee 37831-6122

December 1990

Final Report for Period July 1987-December 1990

Approved for public release; distribution is unlimited.

AERO PROPULSION AND POWER DIRECTORATE
WRIGHT LABORATORY
AIR FORCE SYSTEMS COMMAND
WRIGHT-PATTERSON AIR FORCE BASE, OHIO 45433-6563

NOTICE

When Government drawings, specifications, or other data are used for any purpose other than in connection with a definitely Government-related procurement, the United States Government incurs no responsibility or any obligation whatsoever. The fact that the government may have formulated or in any way supplied the said drawings, specifications, or other data, is not to be regarded by implication, or otherwise in any manner construed, as licensing the holder, or any other person or corporation; or as conveying any rights or permission to manufacture, use, or sell any patented invention that may in any way be related thereto.

This report is releasable to the National Technical Information Service (NTIS). At NTIS, it will be available to the general public, including foreign nations.

This technical report has been reviewed and is approved for publication.

Alan Garscadden

ALAN GARSCADDEN, Research Physicist
Advanced Plasma Research Group
Power Components Branch
Aerospace Power Division

Lowell D. Massie

LOWELL D. MASSIE
Chief, Power Components Branch
Aerospace Power Division
Aero Propulsion and Power Directorate

FOR THE COMMANDER

Michael D. Braydich

MICHAEL D. BRAYDICH, Lt Col, USAF
Deputy Director
Aerospace Power Division
Aero Propulsion & Power Directorate

If your address has changed, if you wish to be removed from our mailing list, or if the addressee is no longer employed by your organization please notify WL/POOC-3, WPAFB, OH 45433-6563 to help us maintain a current mailing list.

Copies of this report should not be returned unless return is required by security considerations, contractual obligations, or notice on a specific document.

SECURITY CLASSIFICATION OF THIS PAGE

REPORT DOCUMENTATION PAGE

Form Approved OMB No. 0704-0188

1a. REPORT SECURITY CLASSIFICATION UNCLASSIFIED	1b. RESTRICTIVE MARKINGS N/A
2a. SECURITY CLASSIFICATION AUTHORITY	3. DISTRIBUTION/AVAILABILITY OF REPORT Approved for public release; distribution is unlimited
2b. DECLASSIFICATION/DOWNGRADING SCHEDULE	
4. PERFORMING ORGANIZATION REPORT NUMBER(S)	5. MONITORING ORGANIZATION REPORT NUMBER(S) WL-TR-91-2019
6a. NAME OF PERFORMING ORGANIZATION Oak Ridge National Laboratory 6b. OFFICE SYMBOL (If applicable)	7a. NAME OF MONITORING ORGANIZATION Aero Propulsion and Power Directorate Wright Laboratory, AFSC
6c. ADDRESS (City, State, and ZIP Code) Oak Ridge Tennessee, 37831-6122	7b. ADDRESS (City, State, and ZIP Code) WL/POOC-3 Wright-Patterson AFB Ohio, 45433-6563
8a. NAME OF FUNDING/SPONSORING ORGANIZATION Air Force Office of Scientific Research 8b. OFFICE SYMBOL (If applicable) NP	9. PROCUREMENT INSTRUMENT IDENTIFICATION NUMBER MIPR FY1455-88-N065
8c. ADDRESS (City, State, and ZIP Code) Bolling AFB Washington D.C. 20332	10. SOURCE OF FUNDING NUMBERS PROGRAM ELEMENT NO. 61102F; PROJECT NO. 2301; TASK NO. S2; WORK UNIT ACCESSION NO. 03
11. TITLE (Include Security Classification) Negative Ion Formation with Electron Impact to Simulants	
12. PERSONAL AUTHOR(S) P.G. Datskos, L.A. Pinaduwage, L.G. Christophorou, & J.G. Carter	
13a. TYPE OF REPORT Final 13b. TIME COVERED FROM 7/87 TO 12/90	14. DATE OF REPORT (Year, Month, Day) December 1990 15. PAGE COUNT 59
16. SUPPLEMENTARY NOTATION	

17. COSATI CODES			18 SUBJECT TERMS (Continue on reverse if necessary and identify by block number)
FIELD	GROUP	SUB-GROUP	Organophosphonates, electron swarm analysis attachment rates, mass spectrometry
20	09		
07	04		

19. ABSTRACT (Continue on reverse if necessary and identity by block number)

The report describes the electron capture properties and ensuing fragmentation pattern of 11 chemical agent simulants: (1) DMMP (2) DIMP (3) nBM (4) 2CLES (5) MS (6) TEP (7) DMP (8) DE3CLMP (9) DECLP (10) DECLMP and (11) DECyMP. The electron attachment coefficient and drift velocity of the negative ions were measured by three techniques (1) time of flight mass spectrometry (2) electron swarm with pulse height analysis and (3) electron swarm with pulsed Townsend method.

20. DISTRIBUTION/AVAILABILITY OF ABSTRACT ☒ UNCLASSIFIED/UNLIMITED ☐ SAME AS RPT ☐ DTIC USERS	21. ABSTRACT SECURITY CLASSIFICATION UNCLASSIFIED
22a. NAME OF RESPONSIBLE INDIVIDUAL ALAN GARSCADDEN	22b. TELEPHONE (Include Area Code) (513) 255-2923 22c. OFFICE SYMBOL WL/POOC-3

DD Form 1473, JUN 86 *Previous editions are obsolete.*

SECURITY CLASSIFICATION OF THIS PAGE
UNCLASSIFIED

Contents

Figures

Tables

Summary

We have studied the electron attachment properties, the fragmentation patterns and the mobilities of the negative ions formed after the collision of slow electrons with 11 different compounds which are simulants for chemical warfare gases.

From the pool of 11 molecules we have found that 5 of them (DMMP, nBM, MS, TEP and DMP) do not capture electrons with energies less than $\sim 1.0\ eV$ (an upper limit for the electron attachment cross section can be placed at $\sim 1.0 \times 10^{-18}\ cm^2$). In a TOF study fragment negative ions were observed for these five molecules for electron energies $> 1.0\ eV$; fairly strong fragment anion formation was detected in this energy range for nBM and DMP.

The original DIMP sample was found to exhibit efficient electron capture at low electron energies but after it was purified with vacuum distillation, electron attachment was considerably reduced. The 2–chloroethyl ehtyl sulfide sample was found to exhibit both dissociative and nondissociative electron attachment. Impurities present in the sample were also responsible for some of the fragment negative ions observed.

DE3ClMP and DEClP were both found to strongly attach electrons ($k_a(\langle\epsilon\rangle) \sim 10^{-9}\ cm^3 s^{-1}$ at thermal electron energies) below $\sim 1.0\ eV$ with electron attachment rate constants that decreased with increasing mean electron energy. Impurity effects were minimal compared to those of other compounds mentioned above. However, DEClP was found to react strongly with Kovar leading to a substantial reduction in the electron attachment.

Impurity effects were also small for DEClMP and DECyMP. However, the electron attachment was ~ 2 orders of magnitude smaller compared to DE3ClMP and DEClP ($k_a(\langle\epsilon\rangle) \sim 10^{-11}\ cm^3 s^{-1}$ at thermal electron energies).

1 Introduction

The present work performed under this contract deals with the study of the electron capture properties and the ensuing fragmentation pattern of 11 chemical war agent gas simulants, namely: (i) DMMP, (ii) DIMP, (iii) nBM, (iv) 2ClES, (v) MS, (vi) TEP, (vii) DMP,(viii) DE3ClMP, (iix) DEClP, (ix) DEClMP and (x) DECyMP.

Knowledge of how and what kind of negative ions are produced when low energy ($\leq 10.0\ eV$) electrons collide with these molecules, as well as the magnitude and electron energy dependance of the electron attachment processes, is of great importance when trying to identify or neutralize these species.

We have measured the electron attachment to the afforementioned compounds and the drift velocity of the negative ions produced by employing three experimental techniques. (i) a time–of–flight mass spectrometer, (ii) an electron swarm technique using a pulse–height–analysis method, and (iii) an electron swarm technique using the pulsed Townsend method.

Chapter 2 contains the description of the experimantal techiques used in the present studies. In Chapters 3 and 4 are presented, respectively, the results and the conclusions of the present study.

2 Experimental Techniques and Procedures

2.1 Electron Swarm Techniques

In electron swarm studies [1],[2] a pulse of electrons emitted at or close to the cathode drifts as an electron swarm under the influence of an applied electric field. The experimental chamber enclosing the electrodes is filled with minute amount ($< 1\ Pa$) of an attaching gas (X) under study mixed with a high pressure ($10 - 100\ kPa$) buffer gas such as N_2 or Ar. The electrons injected at the cathode undergo many collisions with the buffer gas (B) molecules/atoms and quickly attain a steady state electron energy distribution. When $N_X \ll N_B$ (where N_X and N_B are the number densities of the attaching and buffer gas respectively), the steady state electron energy distribution depends on the nature of B and the density–reduced electric field E/N (E is the applied electric field and N is the total gas number density) and can be characterized by the electron energy distribution function $f_B(\epsilon, E/N)$ where $f_B(\epsilon, E/N)d\epsilon$ represents the number of electrons in the energy interval $d\epsilon$ with energy ϵ. After reaching the steady state, the electron swarm drifts towards the anode with a characteristic drift velocity $w = w_B(E/N)$ — when $N_X \ll N_B$ — and may undergo attaching and/or ionizing collisions with the gas X; in the present study the E/N values were low enough so that the electron impact ionization process is ignored. An appropriate buffer gas is chosen so that it is impervious to the drifting electrons and also $f_B(\epsilon, E/N)$ is well known for the range of E/N to be studied; in the present studies N_2 was used. The negative ions formed by the capture of the electrons also drift towards the anode albeit with $\sim$ 1000 times smaller drift velocity compared to that of the electrons. Depending on the particular technique, voltage(s) across a resistor induced by the motion of electrons only, or both electrons and ions were monitored.

2.1.1 Pulse Height Analysis Technique

The Pulse Height Analysis technique used in the present study was devised originally [3] to study electron attachment processes in O_2/Ar mixtures.

In the present study, the electron swarm was produced in a plane at the source electrode, perpendicular to the applied electric field, E, by passage of a high energy α particle through the buffer gas of N_2. The trajectories of these α particles were well collimated so that the electron swarms produced by the ionization of the carrier gas lie in a well defined plane. Each

α particle produced by the decay of Cf^{252} had an energy of $\sim 6.1\ MeV$ and produced a swarm of $\sim 1.7 \times 10^5$ electrons in N_2 within a time of $\sim 5 \times 10^{-9}\ s$ (at a buffer gas pressure of 133 kPa) to $2{\times}10^{-10}\ s$ (at 3.2 MPa).

The experimental apparatus is shown schematically in Fig. 1. The apparatus has been previously described [4] and consists of three parts: (i) the drift chamber, (ii) the gas manifold, and (iii) the carrier gas purification system.

The chamber was pumped by a turbo-molecular pump with a base pressure of a few parts in $10^{-6}\ Pa$, and an outgassing rate of $10^{-2}\ Pa$ per hour. The total (carrier gas) pressure, and that of the attaching gas was measured using a $10,000(\pm 0.1)$ *Torr* and a $1.00000(\pm 0.00001)$ *Torr* MKS Baratron pressure transducer. Using a Bertan (model 205A-10N) programmable power supply (0-20 kV) voltages were applied to the electrodes which were measured by a Keithley (model 182) digital voltmeter, using a high precision voltage divider. The induced anode voltages, produced by the motion of the electrons in the drift region, were detected and amplified by a preamplifier (Tennelec TC 161D) and a linear amplifier (Tennelec TC 222).

The experimental procedure applied in this work was as follows: The chamber was first brought to the desired temperature. At that fixed temperature the pure carrier gas was admitted into the chamber at a given pressure, and a distribution of voltage pulse heights were obtained at a given E/N, which were accumulated in a multichannel analyzer (MCA) operating in the pulse height analysis mode. The most probable pulse height was recorded, the E/N was changed and a new series of most probable pulse heights were obtained as a function of E/N. If the dependence on the total pressure of the attachment processes was also to be studied, then the above sets of measurements were performed over a range of buffer gas pressures as well. An admixture of the attaching gas (usually one part in $10^5 - 10^8$ of the total gas pressure) with the buffer gas was admitted into the chamber, and a new series of most probable pulse heights was obtained as a function of E/N and the total gas number density N_t. Thus by knowing the pulse heights with and without the attaching gas, at any given E/N, the $\eta/N_a(E/N)$ (the attaching-gas-density normalized electron attachment coefficient in units of cm^2) and the $k_a(E/N$ or $\langle\epsilon\rangle)$ (the electron attachment rate constant in units of $cm^3 s^{-1}$) were obtained by using a simple numerical iterative procedure. The partial pressure of the attaching gas was very small, and thus it was assumed that any influence of the attaching gas on the electron energy distribution, $f(\epsilon, \langle\epsilon\rangle)$, was negligible. However, in order to observe and remove any possible such influence, measurements of $k_a(\langle\epsilon\rangle)$ were performed as a function of the attaching gas number density, N_a,

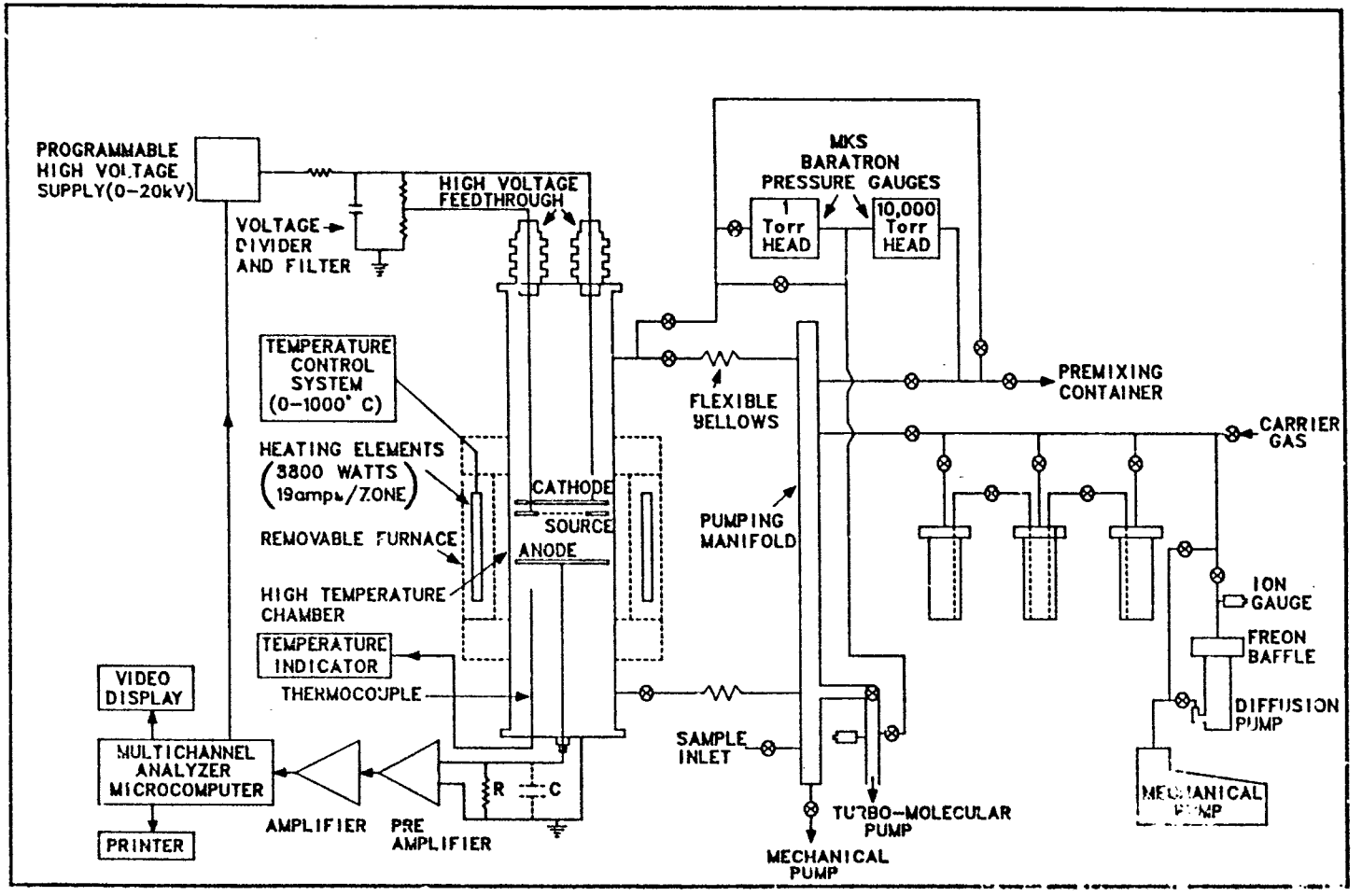

Figure 1: Layout of the pulse height analysis apparatus.

at fixed total gas number densities N_t. From plots of $k_a(\langle\epsilon\rangle)$ N_a/N_t the values of $k_a(\langle\epsilon\rangle)$ for $N_a \rightarrow 0$ were determined by extrapolation. Similar sets of measurements were performed for all the temperatures studied (see Chapter 3).

Before every measurement, the N_2 gas (quoted purity: 99.9995%) was subjected to liquid nitrogen temperatures (for ~ 15 hours) in order to freeze out any condensible impurities (*e.g.*, water vapor) which could affect the voltage pulse heights. The vapor from these gases was then extracted at temperatures just above the boiling point for each buffer gas. This procedure gave stable pulse height measurements which were reproducible to within ± 5 channels in the 2000 channels of the MCA (which is very accurate). The attaching gases used were subjected to several freeze distillation cycles prior to any measurements in order to remove air from the samples. An analysis of the experimental errors in the determination of $k_a(\langle\epsilon\rangle)$ is given [5] in Table 1.

The total uncertainty in $k_a(\langle\epsilon\rangle)$ is estimated to be $\pm 5 - 7\%$. The largest contribution to the error arises from the measurement of the small partial (attaching gas) pressures.

Table 1: Sources of error and their respective estimated uncertainties in the electron swarm experiment

Source	Error
Drift distance	$\pm 1.0\%$
Total gas pressure	$\pm 0.5\%$
Electric field	$\pm 0.5\%$
Partial attaching gas pressure	$\pm 2.0\%$
Electron swarm transit time	$\pm 0.5\%$
Statistical uncertainty in determining the average electron swarm pulse height	$\pm 0.5 - 2.0\%$
Approximation in the numerical iteration procedure to obtain the electron attachment rate constant	Expected to be small when the electron transit time $\ll$ the time constant of the linear amplifier (15 μs)
Non-ideal response characteristics of the linear amplifier	Same conditions as above

2.1.2 Pulsed Townsend Technique

The modified pulsed Townsend technique used in this work has been described earlier [2]. A schematic diagram of the experimental apparatus is depicted in Fig. 2.

The stainless-steel chamber had a base pressure of $\sim 1 \times 10^{-6}$ Pa. Two 10 cm diameter electrodes were mounted in the middle of the chamber using ceramic insulator supports. The bottom electrode was stationary and contained a 4.5 cm diameter quartz insert in the center (Fig. 2); the top surface of the quartz insert was flushed with the electrode surface and the entire surface was coated with a 20 nm gold film. Back illumination of the semitransparent gold cathode by a KrF excimer laser pulse (pulse duration $\sim$ 10 ns, FWHM $\sim$ 10 ns) released a swarm of electrons into the drift region; the electron swarm contained $\sim 10^7$ electrons at a laser pulse energy of ~ 1 mJ.

The anode (top electrode) was connected to a linear motion feedthrough and could be adjusted from outside the vacuum envelope to yield a gap separation, d, (drift distance) between 0 to 5 cm. The voltage induced by the motion of the charged species (electrons and ions) in the drift space was detected at the anode and was fed into a Nicolet 4094C digitizer via an impedance matching (input impedance $\sim 10^{11}$ Ohm), output impedance $\sim$ 50 Ohm unitary gain preamplifier; the rise time of the preamplifier ($\sim$ 5 ns) was less than the laser pulse duration. The digitized data were analyzed in real time using an AT personal computer.

In these measurements a small amount ($\sim$ 1.0 Pa) of the attaching gas was mixed with atmospheric ($\sim$ 100 kPa) N_2 gas. Electron attachment occurred during the drift time t_e of the electrons in the gap, thus producing negative ions. Due to the shorter drift time t_e of the electrons with respect to the time t_- of the negative ions ($t_-/t_e \sim 1000$), the voltage waveform had a "break" (see Fig. 3).

The drift time of the electrons and the drift time of the anions could be deduced from such waveforms. The maximum drift time for negative ions corresponded to the ions which were produced closest to the cathode. Therefore the ionic drift velocity is given by

$$w_- = d/t_- \tag{1}$$

In order to assure that sufficient negative ion formation occurred near the cathode, the attaching gas pressure had to be high enough so that the electron attachment time would be small

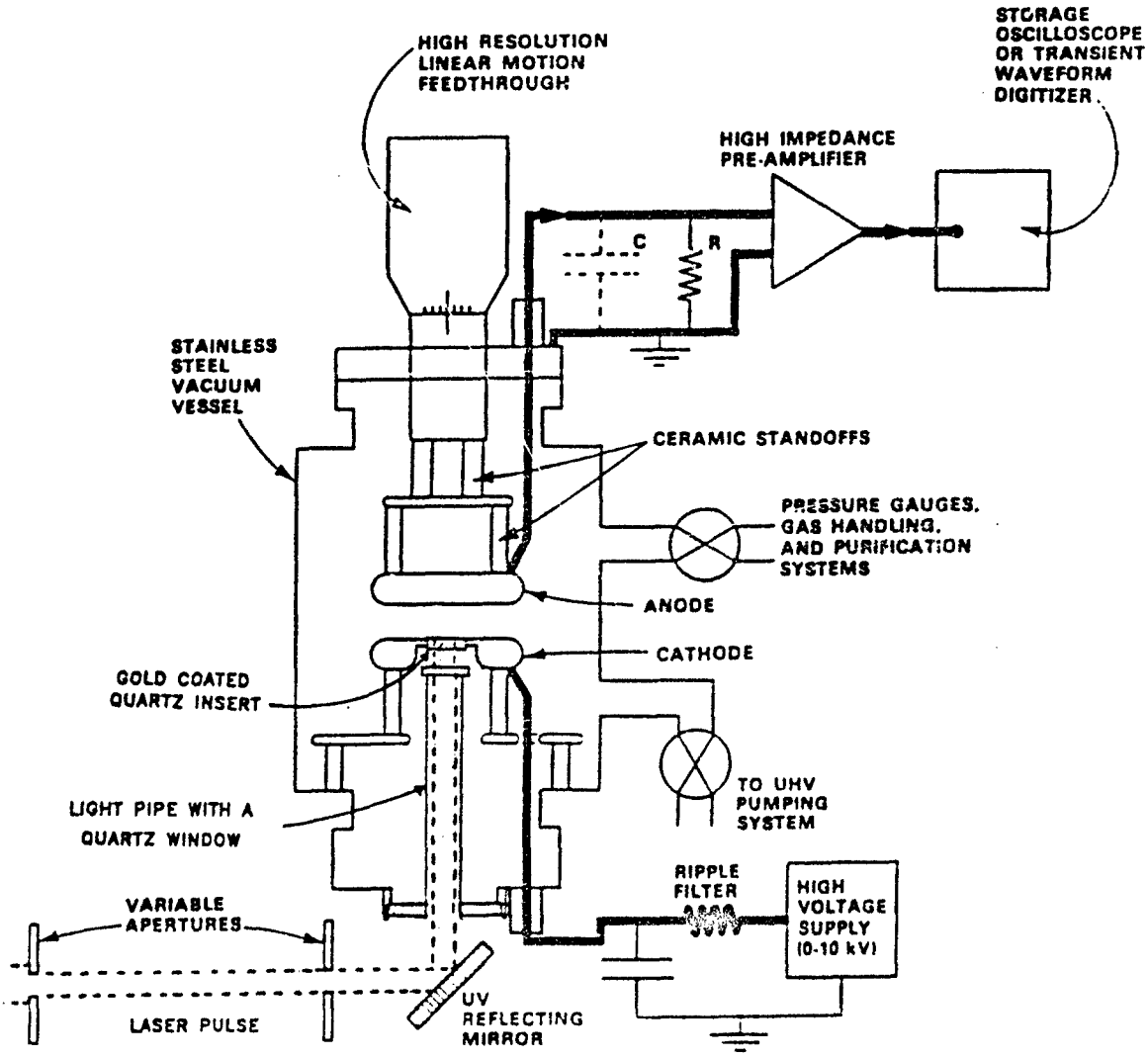

Figure 2: Schematic diagram of the experimental arrangement for the negative ion mobility measurements.

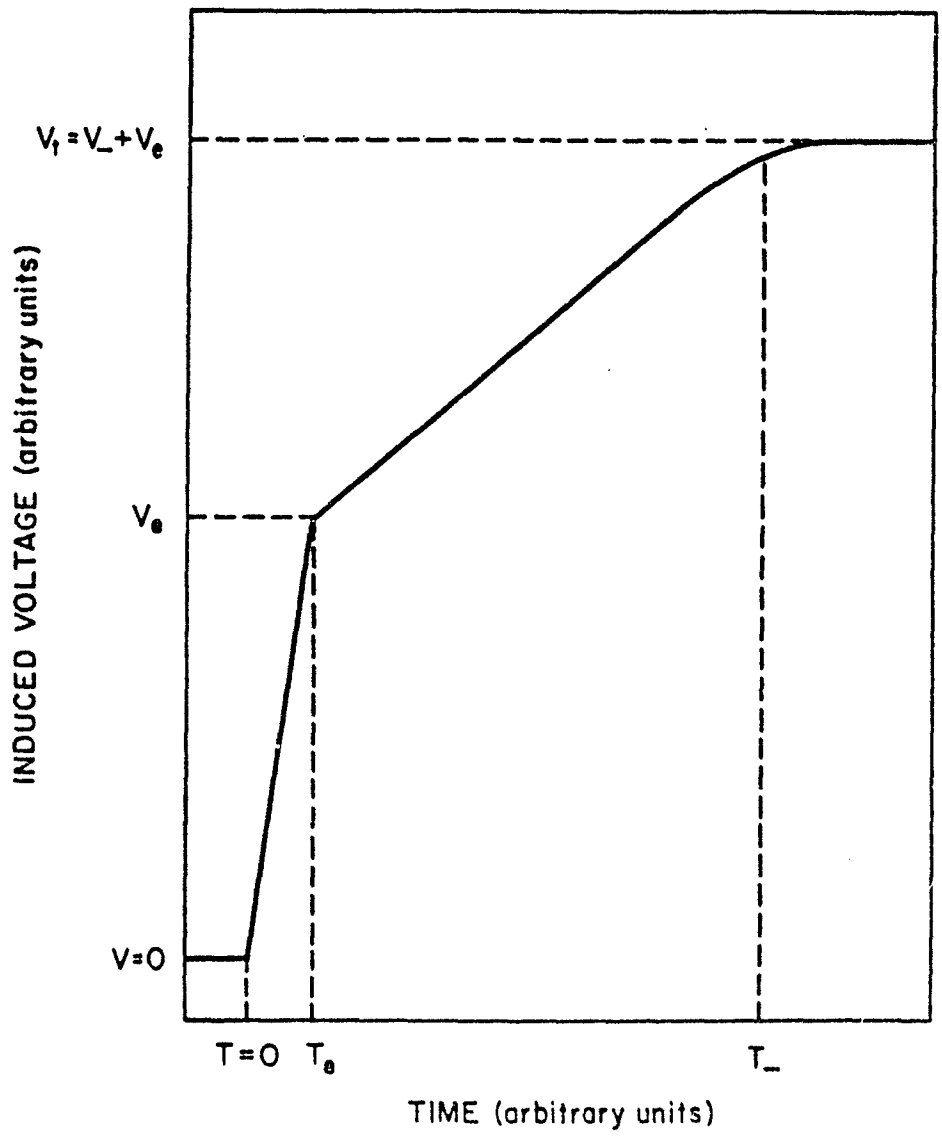

Figure 3: Shematic drawing of a typical waveform. Signal due to the motion of the electrons and ions can be separately measured, and their respective drift times deduced due to the large difference in the drift times of the two species.

compared to t_e, *i.e.*,

$$\frac{1}{N_a k_a} < \frac{d}{w_e}$$

or

$$N_a > \frac{w_e}{d k_a} \tag{2}$$

where N_a and k_a are, respectively, the attaching gas number density and the electron attachment rate constant. The gap separation was kept at its maximum possible value of 5 *cm* in view of the low electron attachment of the molecules under study.

This arrangement lacks the ability to infer the drift velocities for the different anions which could be simultaneously formed; only a "weighted average" drift velocity for all the negative ions produced could be deduced.

2.2 Time–Of–Flight Mass Spectrometer

The TOF mass spectrometer used in this study was constructed at the Oak Ridge National Laboratory and is similar to the Bendix model 14-206. The principles of operation of this type of mass spectrometer have been described earlier [6].

A layout of the entire apparatus is shown in Fig. 4. The TOF can be described as consisting of three parts: (i) the ion source which includes the elecron source ("electron gun") and the collision chamber where the ions are formed, (ii) the flight tube which is the field–free region where the ions are separated by their times–of–flight, and (iii) the detection system which includes the electron multiplier with pulse shaping and pulse selecting electronics. A computer is used to control the electron gun and to measure the pulse rate of the particular ion signal from the electron detection system.

In the ion source the electrons are produced by a heated tugsten filament containing 3% rhenium and is pulsed into the collision chamber through the focusing electrodes (number 1 through 5 in Fig. 4) of the electron gun. The electron gun pulsing is controlled by the first of these electrodes called the anode. The anode is normally negatively biased to turn back all the electrons released by the filament. Every 100 μs a positive pulse of 7 V magnitude and 1 μs duration is applied to the anode to allow electrons to pass through into the collision chamber. Half a μs after the anode pulse, a large negative pulse of 100–200 V and 4 μs duration is applied to the backing plate to push the negative ions (formed when the electrons collided with the gas molecules) into the flight tube. As shown in Fig. 4 the backing plate pulse has a very short "rise" time. A small negative bias has to be continuously applied to the backing plate to compensate for the small positive overshoot of the pulse.

The flight tube (shown in Fig. 4) is a field–free region maintained at a high positive potential (which can be adjusted from 1.0 to 4.5 kV in steps of 0.5 kV) relative to the collision chamber. Negative ions are accelerated to a high kinetic energy as they drift from the position of their formation to the entrance of the flight tube (acceleration grid in Fig. 4), and then travel the length of it at constant velocity.

The detection system is composed of the electron multiplier and associated pulse shaping and pulse electronics; a block diagram is shown in Fig. 4. The electron multiplier is a magnetic–type multiplier (Bendix model M306) which assumes equal detection efficiency for both an ion or a neutral species resulting from electron detachment during the time–of flight. When a species is

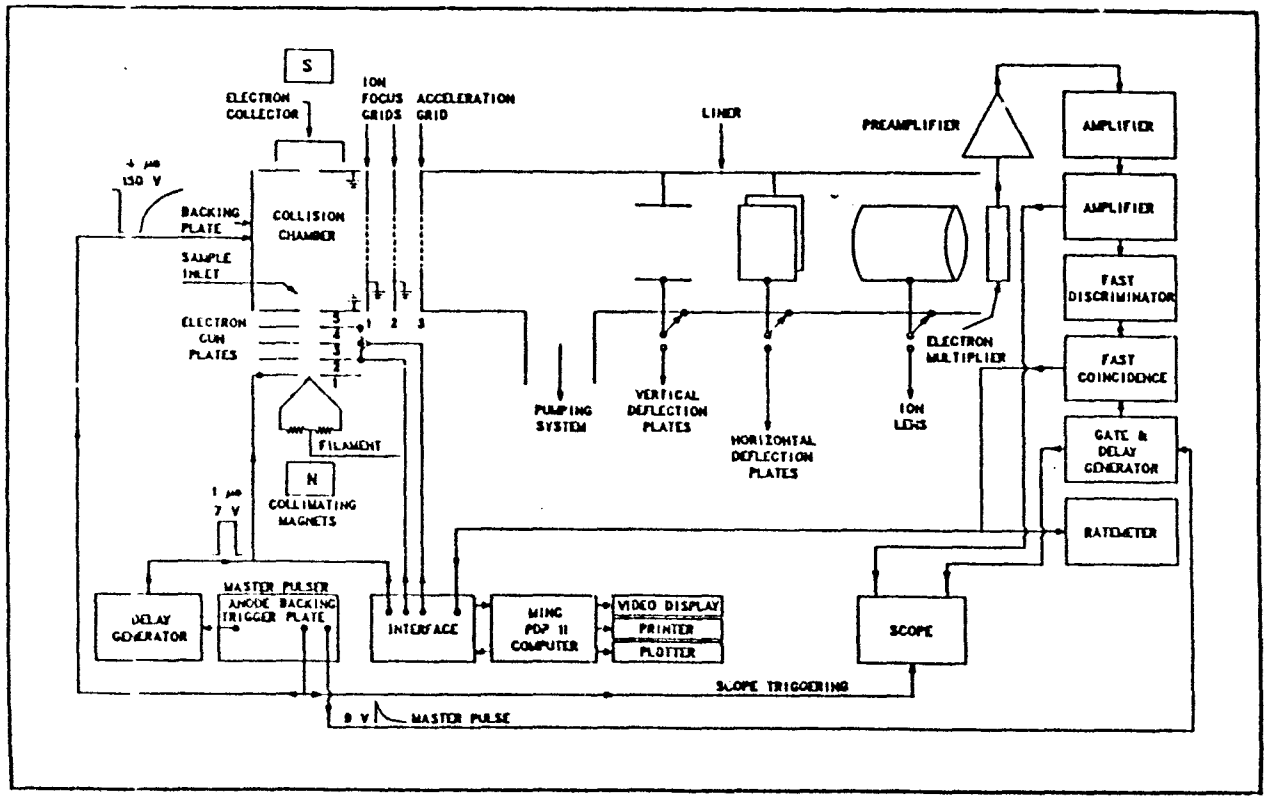

Figure 4: Layout of the time–of–flight mass spectrometer.

detected by the electron multiplier, a pulse is produced which is fed into a high impedance unity gain preamplifier (Keithley model 111) and then into two timing filter amplifiers (ORTEC model 454). The amplified pulse then goes to an oscilloscope and is also fed into a fast discriminator (ORTEC model 417). The discriminator outputs a standard square pulse for every incoming pulse above a certain amplitude. The pulses from the disciminator are fed into a fast coincidence unit (ORTEC model 414A) along with a pulse from a gate and delay generator (ORTEC model 416A) triggered by the "master pulse". The amount of delay is set equal to the flight time of the mass of interest. The coincidence unit then produces a pulse only if the mass signal is received within a selected resolving time of the gate pulse. The output of the coincidence unit represents a signal corresponding to the specific mass, and this signal is counted and recorded.

The spectrometric study of each molecule includes the following stages: (i) mass identification of "all" the negative ions formed from interaction of the electrons with the molecule, and (ii) measurements of the intensity as a function of the electron energy for each anion observed.

Prior to any measurements on any of the molecules under investigation the calibration gas SF_6 was admitted into the collision chamber. Since the electron attachment cross section for SF_6 is very strong and narrow peaking at $\sim 0.0\ eV$, the shape of the SF_6^{-*} resonance was used to monitor the electron energy distribution. To establish the operating conditions of the instrument the procedure described below was followed. First, the filament current was set at $\sim 2.0\ A$ to give a current at the electron collector (Fig. 4) of $\sim 1-3\times10^{-9}$ to $\sim 1-3\times10^{-7}$ A with and without electron pulsing, respectively. Then, the SF_6^{-*} resonance was observed as a function of the electron energy, and the filament current and the backing plate bias were varied until a strong ($\sim$ 4000 *counts/s* at the peak, at a pressure $\sim 1\times10^{-6}$ *Torr*) and a narrow (FWHM $\sim 0.5\ eV$) resonance was obtained.

2.2.1 Mass Identification

After establishing the satisfactory operation of the system the sample molecule was introduced into the interaction chamber. When first trying to identify the anion masses formed for this molecule, the operating pressure was increased to $\sim 1\times10^{-4}$ *Torr*, which is well above the normal operating pressure of $\sim 3\times10^{-5}$ *Torr*. This ensured that weak anions were detected and properly identified (the electron energy was varied from $\sim$ 0.0 to 10.0 eV). In this manner we were able to detect anions whose intensity was as low as one part in one thousand of the

intensity of the strongest negative ion formed from the same molecule. The basic papameter determining the mass separation in the TOF mass spectrometer is the time–of–flight, t, of the ion, given by

$$t = L\sqrt{M/(2E)} \tag{3}$$

where L is the the distance that the negative ion travels, M is its mass, and E is its kinetic energy received on entering the drift tube. Instead of using Eqn (3) to identify the unkown mass we use

$$M_x = M(t_x/T) \tag{4}$$

where M is a known mass, M_x is the unkown mass, T is the time–of –flight of the known mass and t_x that of the unkown. The time–of–flight can be measured with an accuracy of a few tenths of a percent. The strong signal of SF_6^{-*}/SF_6 was used as a calibration mass. The mass determinations were accurate to at least ± 0.3 *amu* for all the ions observed.

2.2.2 Negative Ion Intensity As a Function Of Electron Energy

Once the various negative ions were identified, their relative cross sections as a function of the electron energy were measured. During these measurements the operating pressure was kept low enough so that the intensity of each observed anion varied linearly with pressure; this ensures that no second order processes were involved. Also the peak *counts/s* did not exceed 4000 so that no saturation of the observed signal was occurring.

The electron energy was varied by changing the potential difference between the retarding electrode and the ground. A computer was used to repeatedly scan the electron energy; the gate was set on a particular mass signal and the counts at each electron energy were accumulated until a smooth curve corresponding to the ion intensity as a function of electron energy ϵ was observed. The data had to be first energy calibrated and for this purpose the known resonance SF_5^-/SF_6 was used which peaks at ~ 0.37 *eV*.

3 Results and Discussion

3.1 Dimethyl methyl phoshonate (DMMP)

DMMP was obtained from Pfaltz & Bauer, Inc. with a stated purity of 99.5%. It has a mass of ~ 124 *amu* and its chemical formula is $(CH_3O)_2P(O)(CH_3)$. Its srtuctural formula is represented by

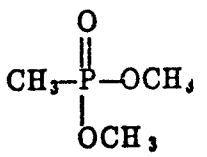

The electron attaching properties of this molecule were investigated by employing the time-of-flight (TOF) and the modified pulsed Townsend (PT) technique (see Chapter 2 for experimental details).

The TOF experiment has shown that five weak fragment negative ions are formed for electron energies from $\sim$ 0.0 up to 14 eV. Negative ions which are formed in collisions of the DMMP molecules with electrons are summarized in Table 2 and are plotted in Fig 5.

Table 2: Formation of negative ions for DMMP in the TOF experiment

Mass (amu)	Negative Ion	Intensity** (Peak counts/s)	Threshold for Electron Attachment	Energy at Which Electron Attachment Peaks (eV)
15	CH_3^-	150	6.3	7.7
78	CH_3OPO^- $[M-OCH_3CH_3]$	90	6.2	7.4
93	$CH_3OP(O)CH_3^-$ $[M-(OCH_3)]$	65	6.7	8.0
62	CH_3PO^-	62	3.6	5.1
	$[M-(OCH_3)_2]^-$ or		6.2	7.4
	$(CH_3O)_2^-$			
31	CH_3O^-	62	6.3	7.9

*M = parent molecule.

**(SF_6^- peak counts/s = 180 x 10^5).

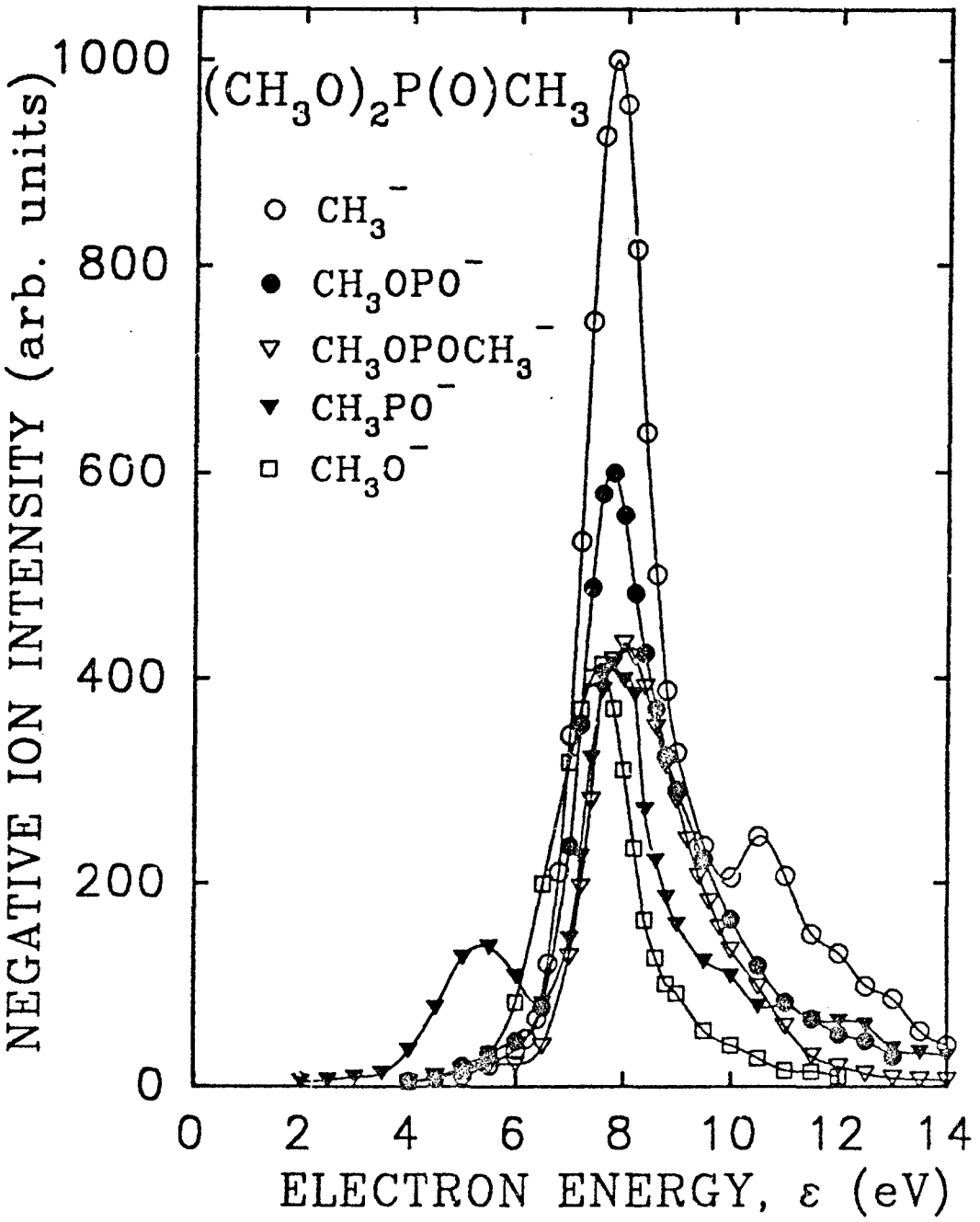

Figure 5: Negative ion intensity as a function of electron energy produced by electron impact on DMMP.

The high pressure ($\sim 100\ kPa$) technique revealed that this molecule attaches very weakly electrons with energies up to $\sim 1.0\ eV$ and the electron attachment rate constant is found to be $< 10^{-13}\ cm^3 s^{-1}$. In particular, this experiment has shown that no significant negative ions are formed in N_2 ($E/N \leq 1.0 \times 10^{-16}\ Vcm^2$) and in Ar ($E/N \leq 1.0 \times 10^{-16}\ Vcm^2$) which translates into an upper limit for the overall electron attachment cross section of $\sim 10^{-18}\ cm^2$. However, positive ion formation (ionization of DMMP) was observed in Ar above $E/N \sim 1.0 \times 10^{-17}\ Vcm^2$. For this E/N the mean electron energy is $\sim 10\ eV$ which corresponds roughly to the ionization threshold of DMMP.

We have also found that addition of water to DMMP in N_2 does not increase the electron attachment to DMMP. The same was observed when the temperature of the sample was increased from 25 $°C$ to 50 $°C$.

3.2 Diisopropyl methyl phoshonate (DIMP)

DIMP was obtained from Alfa Chemical company with a stated purity of 98%. It has a mass of ~ 180 *amu* and its chemical formula is $CH_3P(O)(i\text{-}OC_3H_7)_2$. Its structural formula is represented by

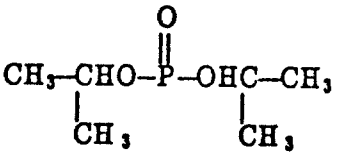

In the TOF study two negative ion fragments with masses of 126 and 138 *amu* respectively were produced. The anion with a mass of 126 *amu* was the strongest with a resonance at ~ 0.0 *eV* (see Fig. 6 and Table 3). The mass 138 *amu* anion was barely detectable and it exhibited a peak at ~ 3.0 *eV*. The fragment with mass of 126 *amu* cannot be attributed to a simple fragment of DIMP. It is possible that it was due to impurities present in the sample. According to the manufacturer the major impurity would be tri-isopropyl-phosphite (from which however, a simple fragment with mass 126 *amu* cannot be identified). Also, according to the manufacturer if the sample was old, a decomposition product P_2O_4 is likely to be formed. The mass of the fragment P_2O_4 is 126 *amu* and therefore P_2O_4 is a strong candidate for the unidentified resonance with mass 126 *amu*. In order to verify this possibility, DIMP was vacuum distilled. Since P_2O_4 is a solid powder it should have been removed during the vacuum distillation. But when the experiment was repeated with the "purified" sample the same resonance with a mass of 126 *amu* was still present and the results of the distilled and undistilled sample were virtually identical. After this we performed a gas chromatographic analysis which revealed the presence of two impurities of masses 165 and 181 *amu* respectively which were tentatively identified as $(C_3H_7O)_2P(O)O$ and $(C_3H_7O)_2P(O)OH$. The anion with mass 126 *amu* could not be identified as a simple fragment of any of these impurities.

We found that the negative ion intensity due to the fragment anion with mass of 138 *amu* increased with increasing temperature. This then indicates that it is due to some decomposition product of DIMP. This fragment anion can be tentatively identified as $C_3H_7OCH_3(PO)OH^-$.

The electron attachment coefficient, η/N_a, of DIMP was also measured using the PT tech-

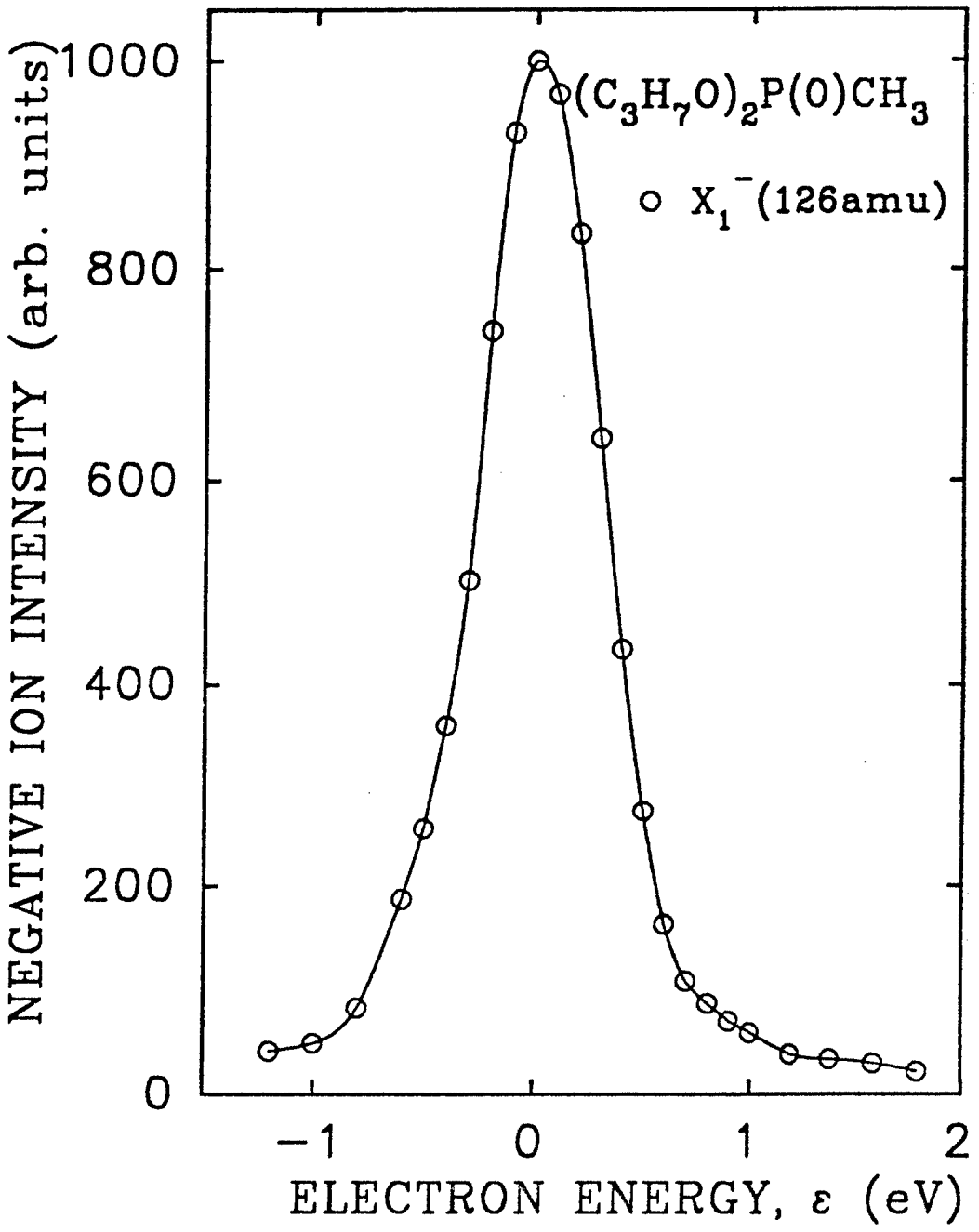

Figure 6: Negative ion intensity as a function of electron energy produced by electron impact on DIMP.

Table 3: Formation of negative ions for DIMP in the TOF experiment

Mass (amu)	Negative Ion	Intensity* (Peak counts/s)	Energy at Which the Resonance Peaks (eV)
126^{+}	X_1^-	40×10^5	~0.0
138	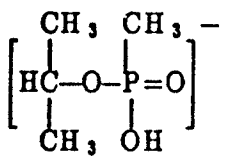	$< 1 \times 10^2$	~3.0

*(SF_6^- peak counts/s = 180×10^5).

+This negative ion is probably due to impurities in the sample.

nique before and after the distillation and the results are plotted in Fig. 7. Before the vacuum distillation apart from the peak at $\sim 0.0\ eV$ ($E/N \sim 1.0 \times 10^{-19}\ Vcm^2$), a second peak was observed at $\sim 0.4\ eV$ ($E/N \sim 1.0 \times 10^{-17}\ Vcm^2$). The electron attachment coefficient at $\sim 0.0\ eV$ was independent of the N_2 pressure indicating fragment negative ion formation (dissociative electron attachment) and is consistent with the TOF measurements. On the other hand the second peak at $E/N \sim 1.0 \times 10^{-19}\ Vcm^2$ was dependent on N_2 pressure (see Fig. 7 and 8) indicating parent ion formation with N_2 acting as the stabilizing third body.

After the purification the η/N_a was smaller overall, but, more signifigantly, the N_2- pressure-dependent electron attachment disappeared (see Fig. 7). Therefore, it seems that the N_2-pressure-dependent electron attachment process was due to some impurity present in the original sample. Note that the TOF experiment is carried out under low pressure ($\sim 10^{-3}\ Pa$) and therefore this electron attaching process would not have been observed in that experiment.

The weaker resonance observed in the TOF study appeared at $\sim 3.0\ eV$ and mean electron energies of $\sim 3.0\ eV$ are not accessible in the swarm study when using N_2 as a buffer gas.

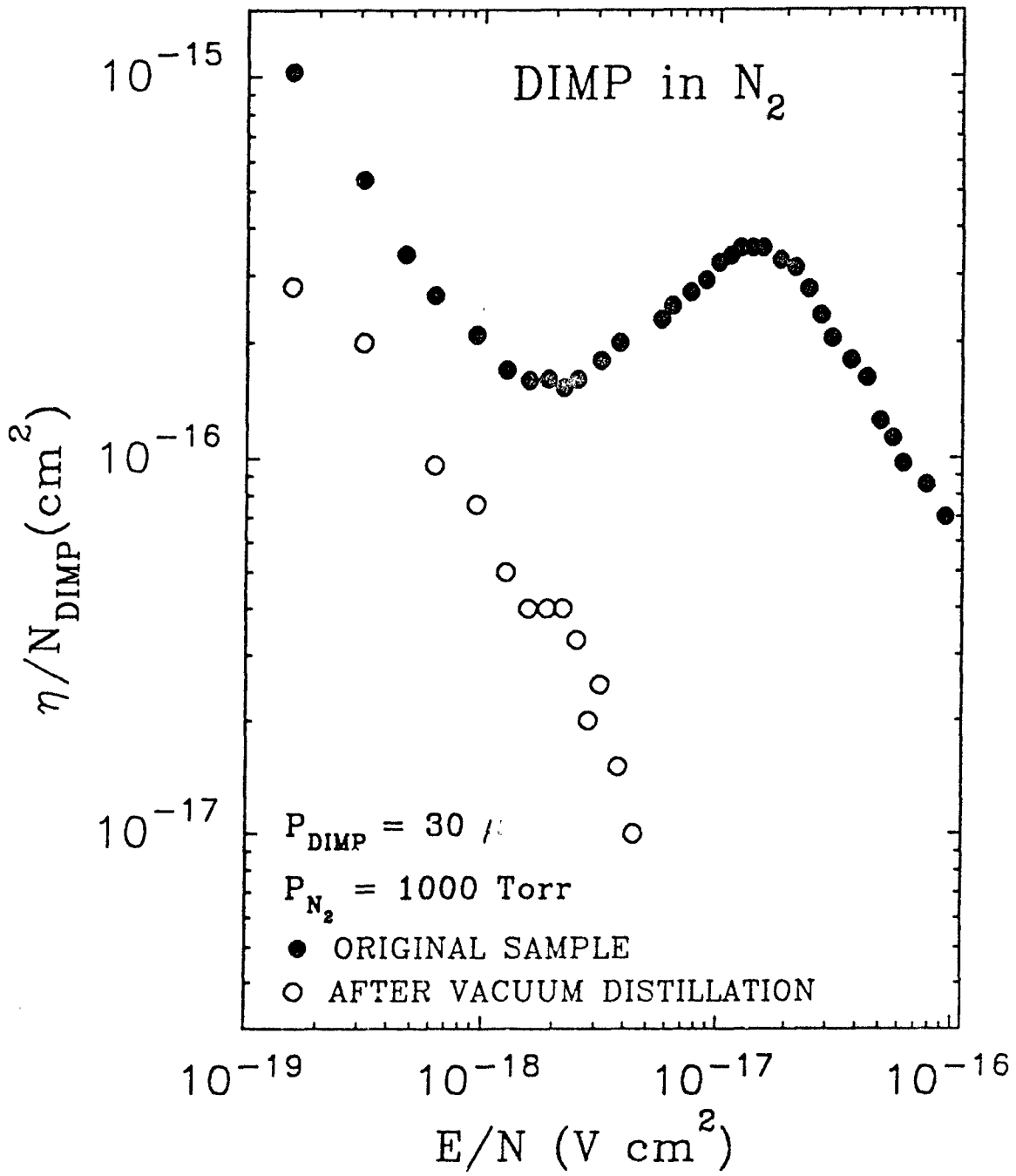

Figure 7: Electron attachment coefficient as a function of E/N for DIMP.

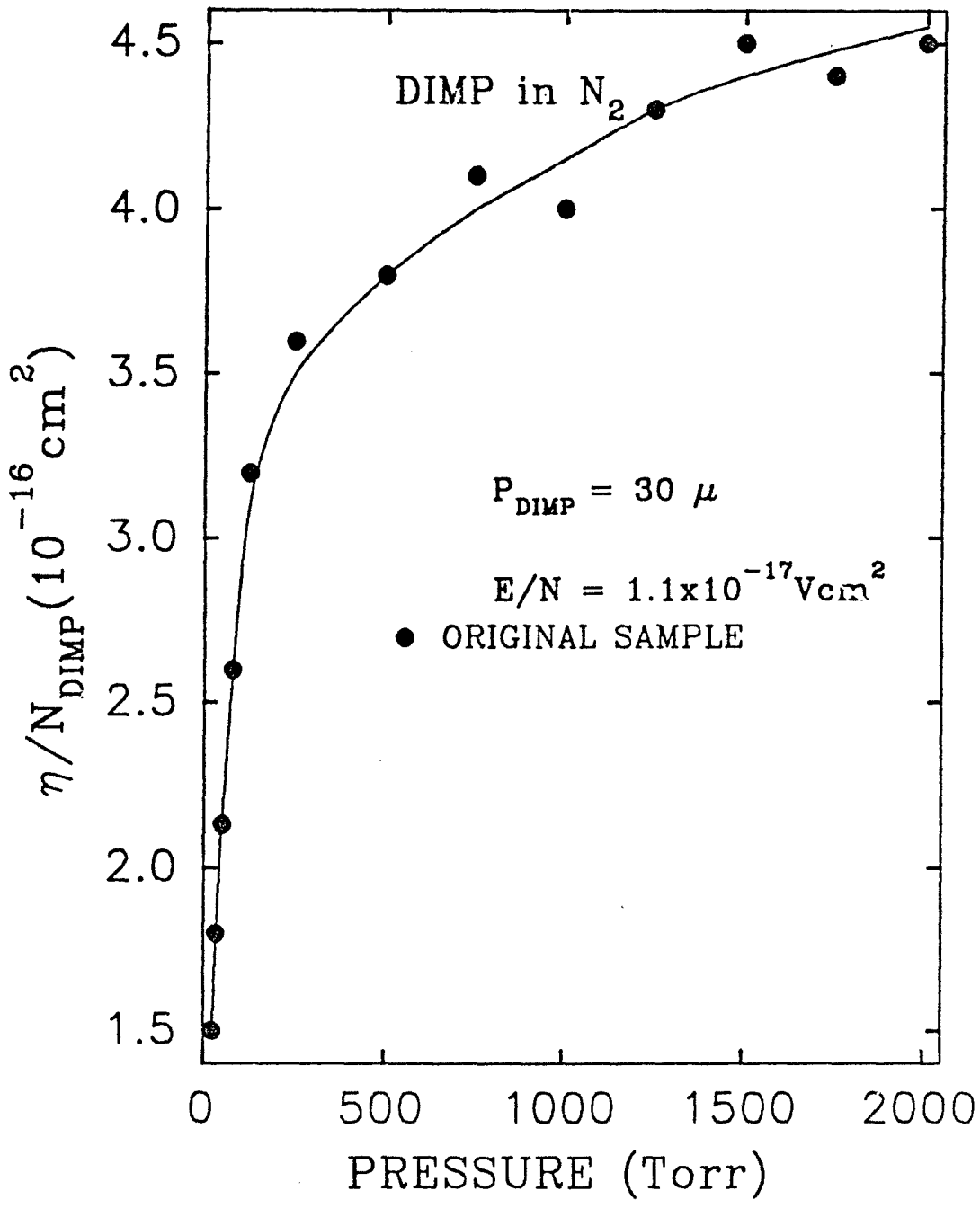

Figure 8: Electron attachment coefficient as a function of P_{N_2} for DIMP.

3.3 n-Butyl mercaptan (nBM)

n-Butyl mercaptan was obtained from Aldrich Chemical company with a stated purity of $99+\%$. It has a mass of ~ 90 *amu* and its chemical formula is $(CH_2)_3CH_3SH$. Its structural formula is represented by

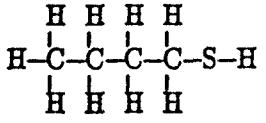

In the TOF study six negative ions were observed for electron energies in the range of ~ 0.0 to 10 eV and are plotted in Fig. 9 and are summarized in Table 4.

In the PT study a weak electron attachment ($\eta/N_a \sim 5.0 \times 10^{-18} cm^2$) was observed in the E/N range of $\sim 6.0 \times 10^{-18}$ to $\sim 2.5 \times 10^{-17}$ Vcm^2 ($\langle\epsilon\rangle$ from 0.23 to ~ 0.65 eV) in early runs. However, after repeating several freeze–pump–thaw purification cycles this electron attachment disappeared. Comparing with data from the TOF measurements we can tentatively identify this imputiry as ethyl mercaptan.

At ~ 0.0 eV another electron attachment process was observed which was also very weak and decreased rapidly with increasing $\langle\epsilon\rangle$ (see Fig. 10). For this process no dependence was observed on either the attaching gas or the buffer (N_2) gas pressure. This indicates that this is a dissociative electron attachment process and can be identified with the dissociative electron attachment observed in the TOF study which involves the SH^- ion. The dissociative electron attachment processes observed at electron energies > 1.0 eV cannot be observed in the swarm experiment using N_2 buffer since the mean electron energy does not exceed ~ 1.0 eV.

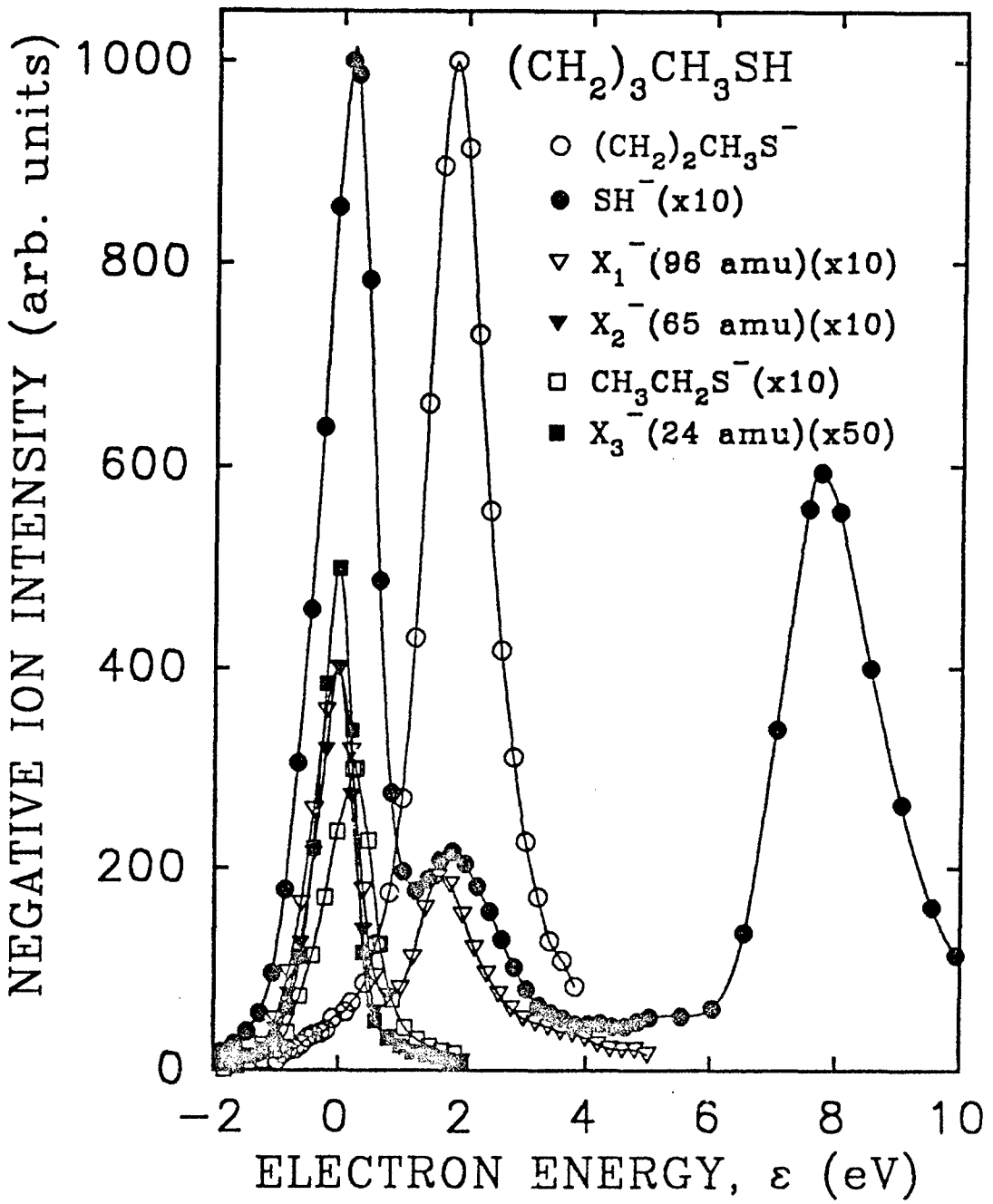

Figure 9: Negative ion intensity as a function of electron energy produced by electron impact on n-butyl mercaptan.

Table 4: Formation of negative ions for n–butyl mercaptan in the TOF experiment

Mass (amu)	Negative Ion	Intensity*	Energy at Which the Resonance Peaks (eV)
89	$CH_3CH_2CH_2CH_2S^-$	$2x10^{-3}$	1.82
33	SH^-	$2x10^{-4}$ $4x10^{-5}$ $1.2x10^{-4}$	~0.0 ~2.0 ~7.9
96	X_1^-	$8x10^{-5}$ $4x10^{-5}$	~0.0 1.7
65	X_2^-	$8x10^{-5}$	~0.0
61^+	$CH_3CH_2S^-$	$6.5x10^{-5}$	~0.28
24	X_3^-	$2x10^{-5}$	~0.0

*Relative intensity = 1 for SF_6^- ion at ~0.0 eV at the same pressure as that of n–butyl mercaptan.

+This could be attributed to the presence of ethyl mercaptan as an impurity produced by recombination of fragment ions of n–butyl mercaptan.

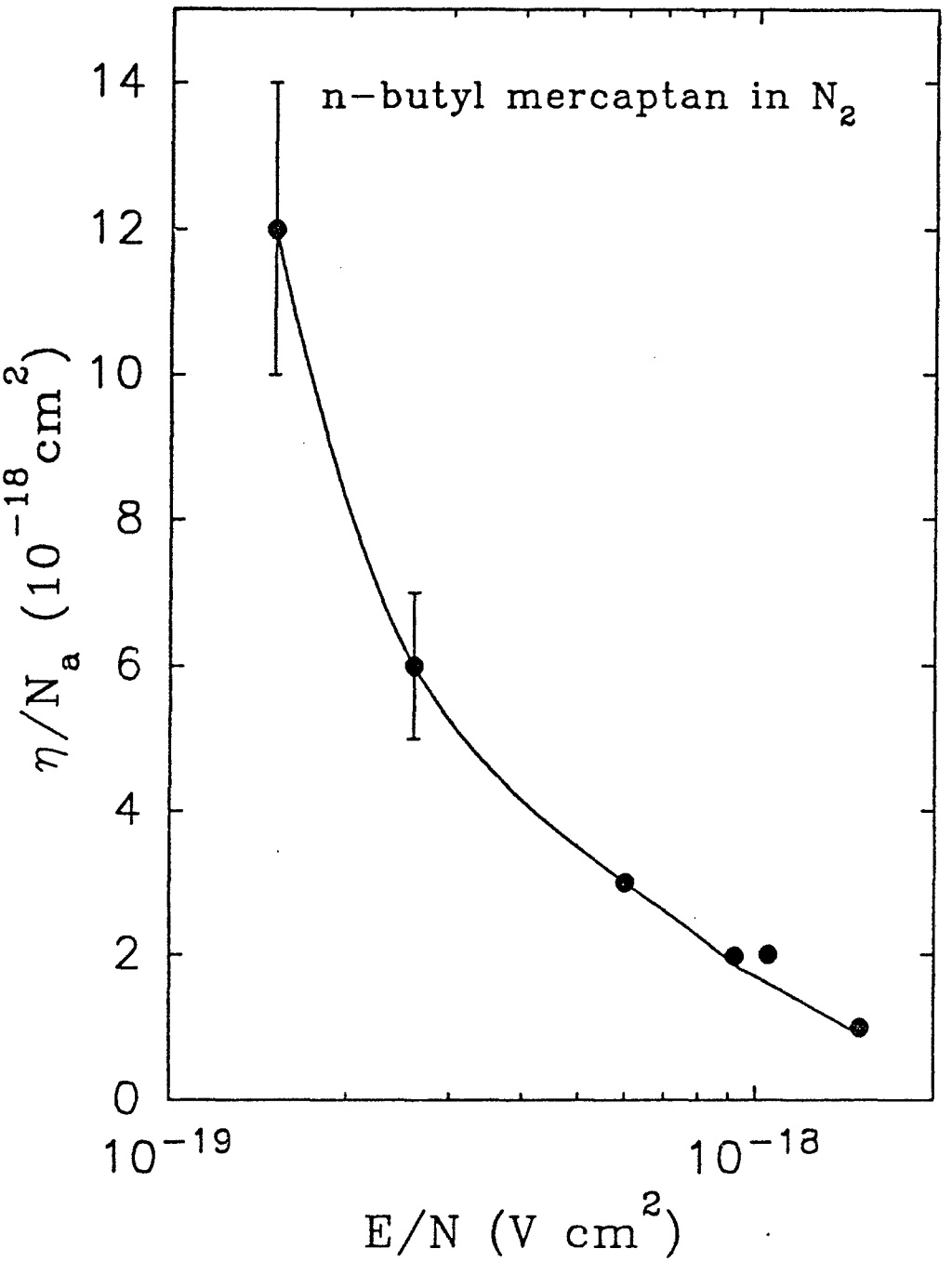

Figure 10: Electron attachment coefficient as a function of E/N for n-butyl mercaptan.

3.4 2–Chloroethyl ethyl sulfide (2ClES)

2–Chloroethyl ethyl sulfide was obtained from Aldrich Chemical company with a stated purity of 99%. It has a mass of $\sim$ 124 *amu* and its chemical formula is $(CH_2)_2C_2H_5SCl$. Its structural formula is represented by

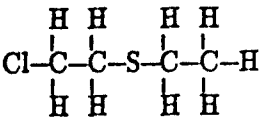

In the time–of–flight study initially an anion with a mass of 48 *amu* (perhaps from methyl mercaptan) was observed peaking at $\sim$ 1.0 and at 5.38 eV. However, after pumping on the sample for 10-15 hours it disappeared, which leads to the conclusion that it was an impurity. The other negative ions detected are summarized in Table 5 and are plotted in Fig. 11.

This sample was also studied using both the (PT) and the (PHA) experiments. In both these experiments it was not possible to obtain consistently reproducible results. Results for the electron attachment coefficient, η/N_a, obtained from these two experiments are shown in Fig. 12. We can see that there are two peaks; one at $E/N \rightarrow 0$ ($\sim$ 0.0 eV) and another at an E/N of $\sim 1.2 \times 10^{-17}$ $V\ cm^2$ which corresponds to a mean electron energy of $\sim$ 0.4 eV. The two resonances were always present; however, their relative intensities as well as their absolute magnitudes varied between successive runs. Repeated freeze–pump–thaw cycles did not improve this situation. This may indicate the presence of an impurity with a vapor pressure nearly equal to that of 2-chloroethyl ethyl sulfide.

It was also observed that when the same mixture of attaching/buffer gas was left in the chamber for several hours there was no time dependence of the measurements. Therefore, the changes in the measured values must occur due to the changes in the percentage of the impurity entering the vessel in different fills. Using the same 2–chloroethyl ethyl sulfide number density and adding more and more buffer gas in successive runs the dependence of η/N_a on the total number gas density was measured. This revealed that η/N_a was independent of the total gas number density at the higher electron energy ($\langle\epsilon\rangle \sim 0.4\ eV$), while the peak at $\sim$ 0.0 eV increases with increasing total number gas density. This indicates that this sample captures

Table 5: Formation of negative ions for 2–chloroethyl ethyl sulfide as measured in the TOF experiment

Mass (amu)	Negative Ion	Relative Intensity*	Energy at Which the Resonance Peaks (eV)
35	Cl^-	$2x10^{-3}$	~0.34
33	SH^-	$1.3x10^{-4}$	~0.36
96^+	$CH_2Cl–S–CH_3^-$	$1x10^{-4}$	~0.37
61	$CH_3CH–S^-$	$5x10^{-5}$ $1x10^{-5}$ $2.5x10^{-5}$	~0.51 ~0.53 ~0.74

*Relative intensity with respect to SF_6^- which is 1 at ~0.0 eV under identical conditions and pressure.

+This could also be due to the presence of chloromethyl methyl sulfide as an impurity.

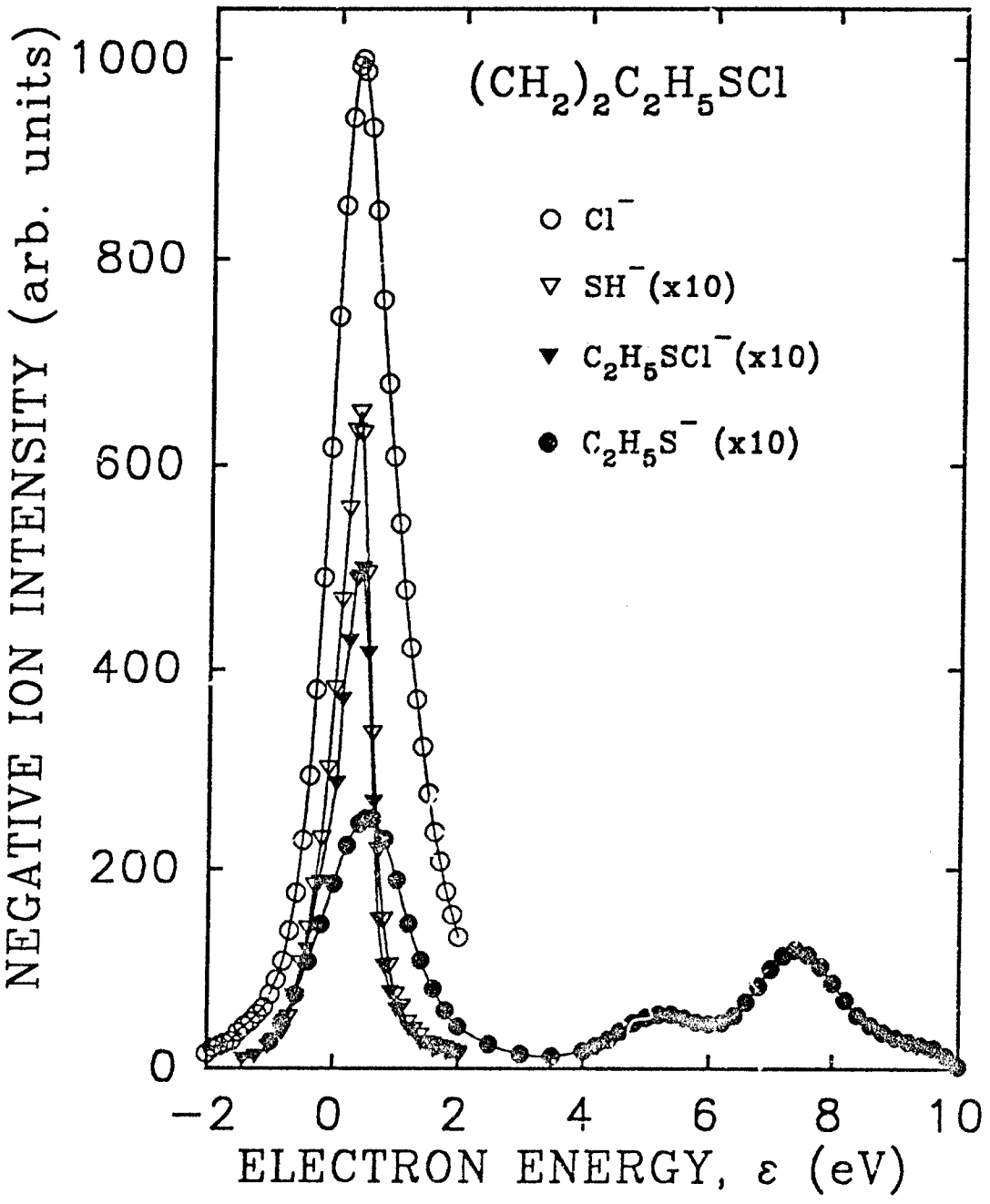

Figure 11: Negative ion intensity as a function of electron energy produced by electron impact on 2–chloroethyl ethyl sulfide.

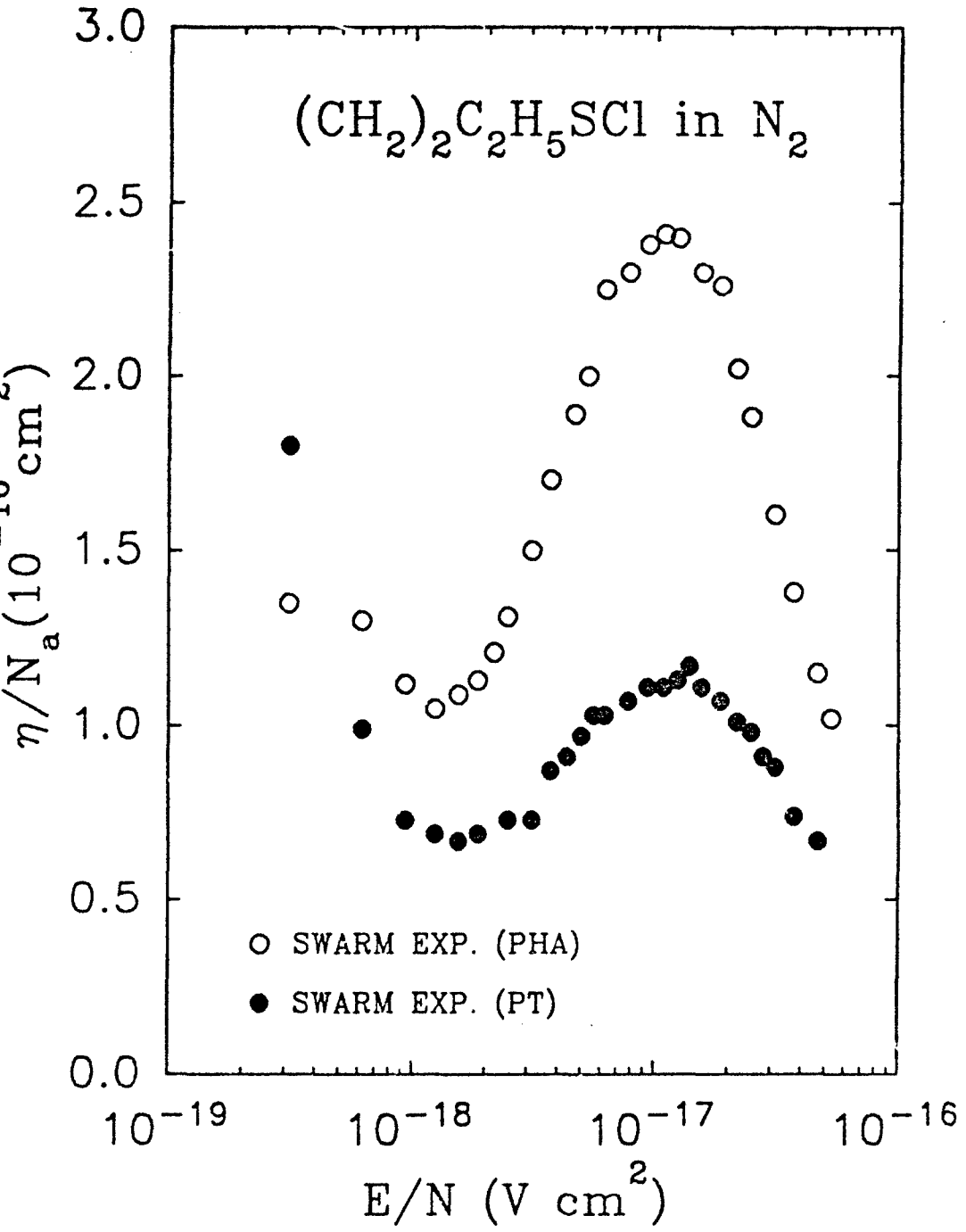

Figure 12: Electron attachment coefficient as a function of the density reduced electric field for 2-chloroethyl ethyl sulfide.

electrons nondissociatively at $\sim 0.0\ eV$ and dissociatively at $\sim 0.4\ eV$.

The above observations are in agreement with the results from the TOF study. The TOF study shows three dissociative electron attachment processes around $\epsilon \sim 0.4\ eV$. Since the anion with mass 96 *amu* observed in the TOF apparatus at $\sim 0.37\ eV$ could be due to the presence of chloromethyl methyl sulfide as an impurity, this then may be responsible for the variations in η/N_a at $\sim 0.4\ eV$ observed in the electron swarm experiments. The resonance at $\sim 0.0\ eV$ is due to parent anion formation (nondissociative electron attachment) and therefore would not be detectable in the TOF apparatus.

In conclusion, we can say that: (i) the process at $\sim 0.0\ eV$ is due to parent ion formation processes involving partly or totally an impurity; (ii) the peak observed at $\sim 0.4\ eV$ in the electron swarm experiments is due to several dissociative electron attachment processes one of which involves an impurity which could be chloromethyl methyl sulfide. However, a gas chromatographic analysis did not reveal the presence of chloromethyl methyl sulfide but it revealed the presence of an impurity with a mass of 148 *amu* which can be tentatively identified as methyl ester or ethyl sulfide. The electron attaching properties of these compounds are not known.

3.5 Methyl salicylate (MS)

MS was purchased from Aldrich Chemical company with a purity of $99+\%$. It has a mass of ~ 110 *amu* and its chemical formula is 2-$(OH)C_6H_4(CO)_2(CH_3O)$. Its structural formula is represented by

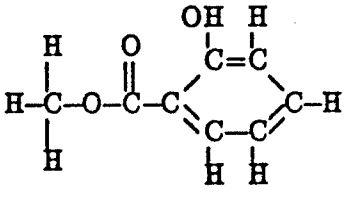

The electron attachment properties of MS were studied using the PHA and the PT experiment in a buffer gas of N_2 at a total pressure of 100 kPa and over the mean electron energy range ~ 0.0 to ~ 0.9 eV. In this energy range MS is a weak electron attacher and these studies have placed an upper limit to the electron attachment rate constant at $\sim 10^{-14}$ cm^3s^{-1}.

In The TOF study three negative ions were observed and identified in the electron energy range ~ 1.0 to 7.0 eV. The results are summarized in Table 6 and are plotted in Fig. 13.

Table 6: Formation of negative ions for MS as measured in the TOF experiment

Mass (amu)	Negative Ion	Relative Intensity*	Peak Position (eV)
137	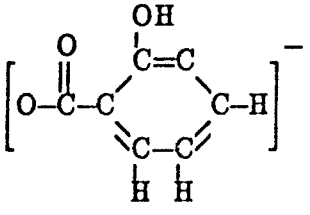	2.3×10^{-4}	1.27
93	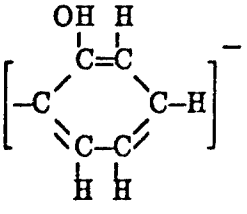	4×10^{-4}	6.14
31	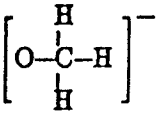	2.6×10^{-4}	6.57

*Relative intensity with respect to that ($\equiv 1$) for SF_6^- at 0.0 eV at the same pressure as MS.

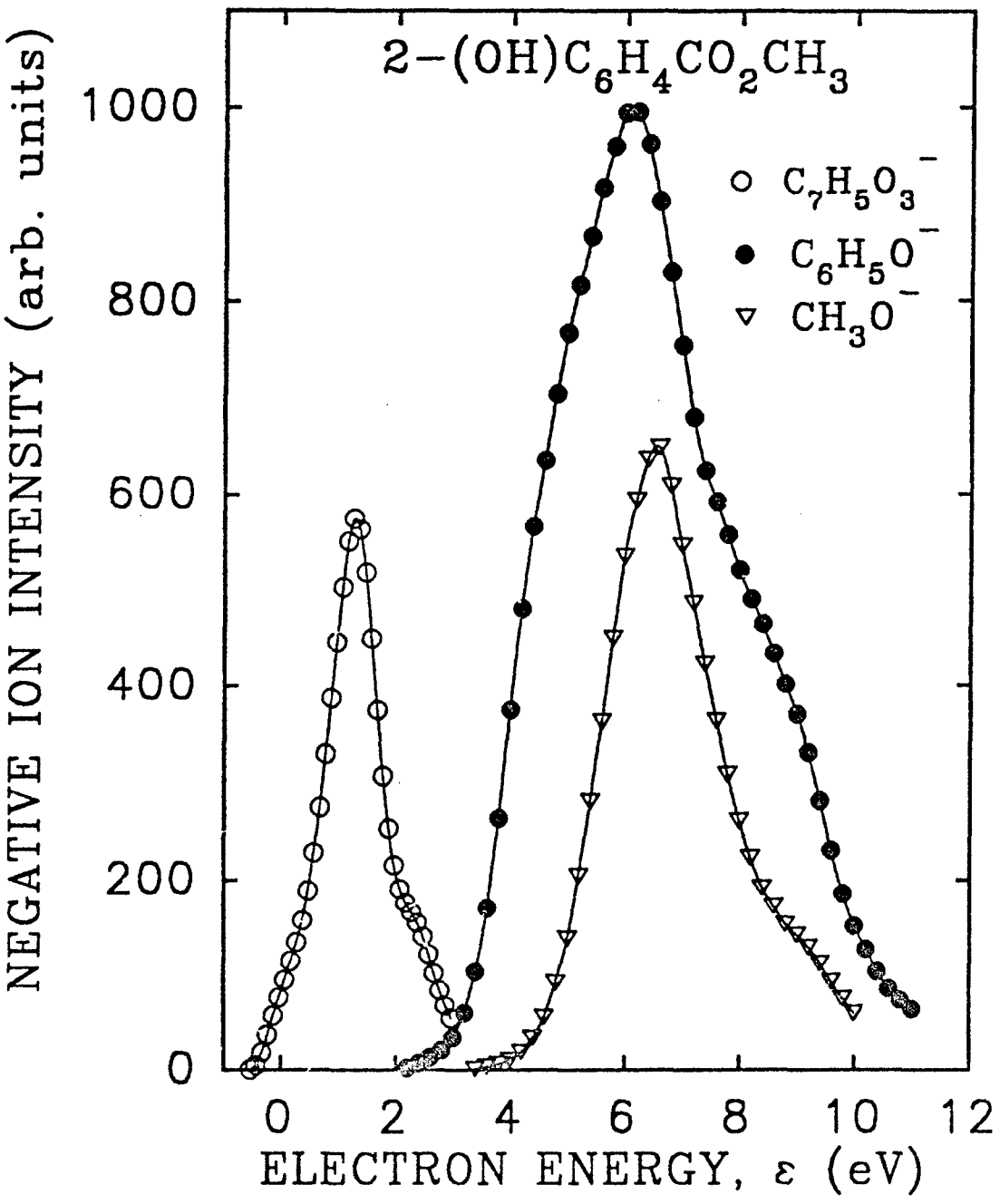

Figure 13: Negative ion intensity as a function of electron energy produced by electron impact on MS.

3.6 Triethyl phoshate (TEP)

TEP was purchased from Aldrich Chemical company with a purity of 99+%. It has a mass of ~ 182 *amu* and its chemical fomula is $(C_2H_5O)_3(PO)$. Its structural formula is represented by

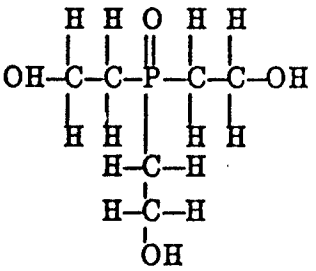

In the TOF experiment only one fragment negative ion was observed and identified. It had a mass of 153 *amu* and had a resonance at ~ 2.8 *eV* (see Table 7 and Fig. 14). However after the vapor of TEP was passed through the TOF apparatus for more than ~ 30 minutes another negative ion appeared at ~ 0.0 *eV* with a mass of 238 *amu*. This mass is larger than that of the parent molecule (TEP). The negative ion intensity due to this species increased when the ion gauge which monitors the pressure of the attaching gas (TEP) was heated, which indicates an enhancement of a reaction of TEP with the hot filament of the ion gauge.

TEP was also studied in the electron swarm experiment (PHA) in a buffer gas of N_2 at a pressure of ~ 1 *atm* and it showed that there is no measurable electron capture in the mean electron energy range, $\langle\epsilon\rangle \sim 0.0$ to ~ 0.9 *eV*. This, then, puts an upper limit on the electron attachment rate constant k_a of $\sim 10^{-14}$ cm^3s^{-1}.

Table 7: Formation of negative ions for TEP as measured in the TOF experiment

Mass (amu)	Negative Ion	Relative Intensity*	Peak Position (eV)
153	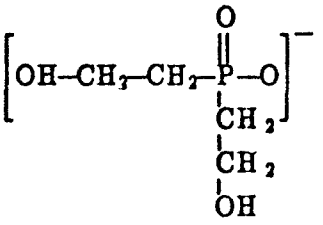	6×10^{-5}	2.8

*Relative intensity is 1 for SF_6^- at 0.0 eV at the same pressure as TEP.

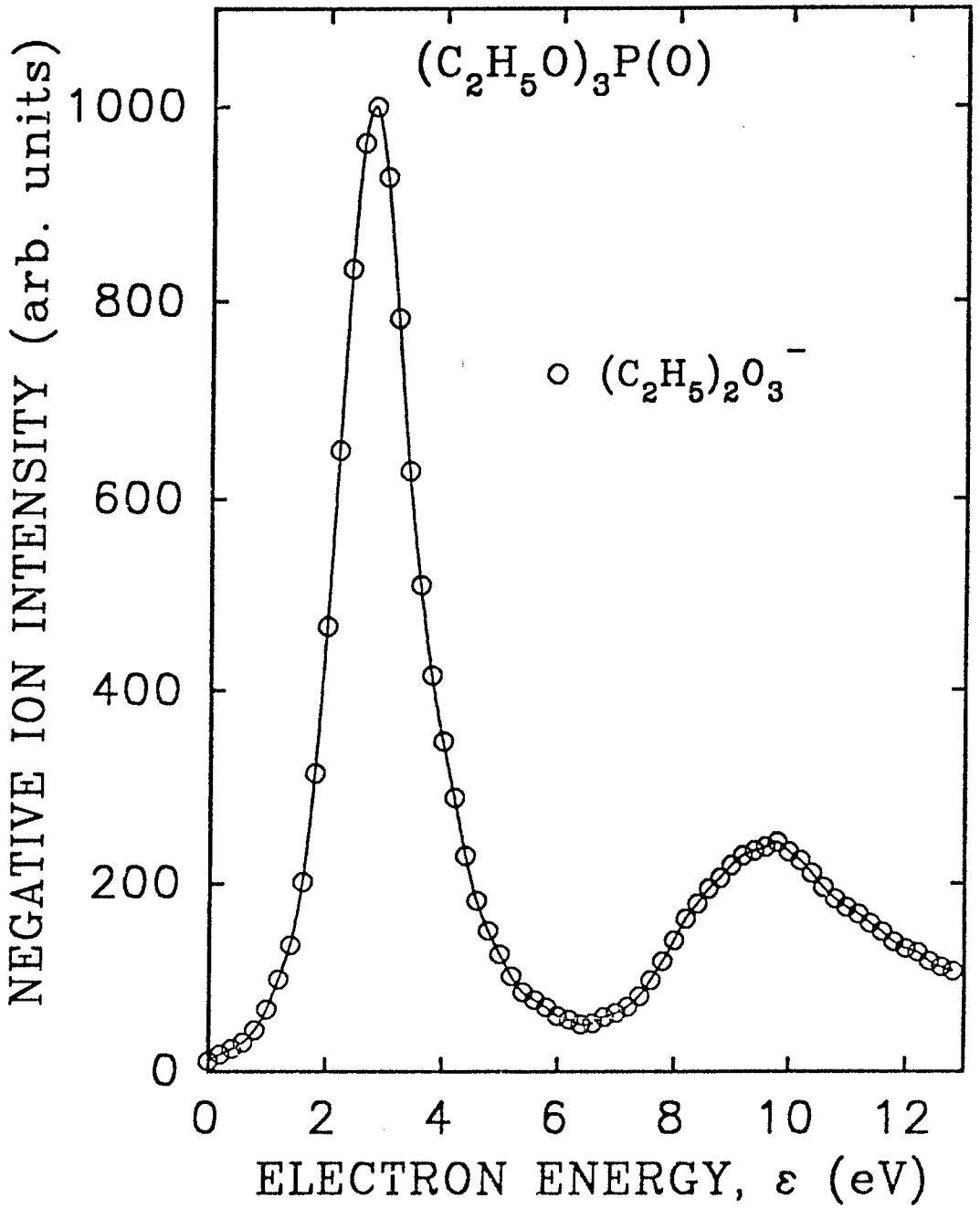

Figure 14: Negative ion intensity as a function of electron energy produced by electron impact on TEP.

3.7 Dimethyl phoshite (DMP)

DMP was obtained from Aldrich Chemical company with a purity of 99 + %. It has a mass of $\sim$ 110 *amu* and its chemical fomula is $(CH_3O)_2P(OH)$. Its structural formula is represented by

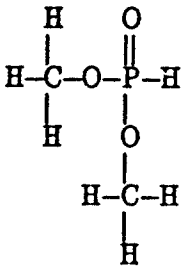

In the TOF experiment DMP formed only one fragment negative ion at $\sim$ 2.5 eV with a mass of 109 *amu*. The TOF results are shown in Fig. 15 and are summarized in Table 8. DMP also was found to react with the hot filament of the ion gauge; an anion with a mass of 165 *amu* was observed at $\sim$ 0.0 eV after the filament was heated.

DMP was also studied by employing the PHA electron swarm technique in a buffer gas of N_2 and a pressure of $\sim$ 1 *atm*. This study has revealed that there was no measurable electron attachment in the mean electron energy range of $\langle\epsilon\rangle \sim 0.0$ to ~ 0.9 eV. This, then, puts an upper limit on the electron attachment rate constant k_a of $\sim 10^{-14}$ cm^3s^{-1}.

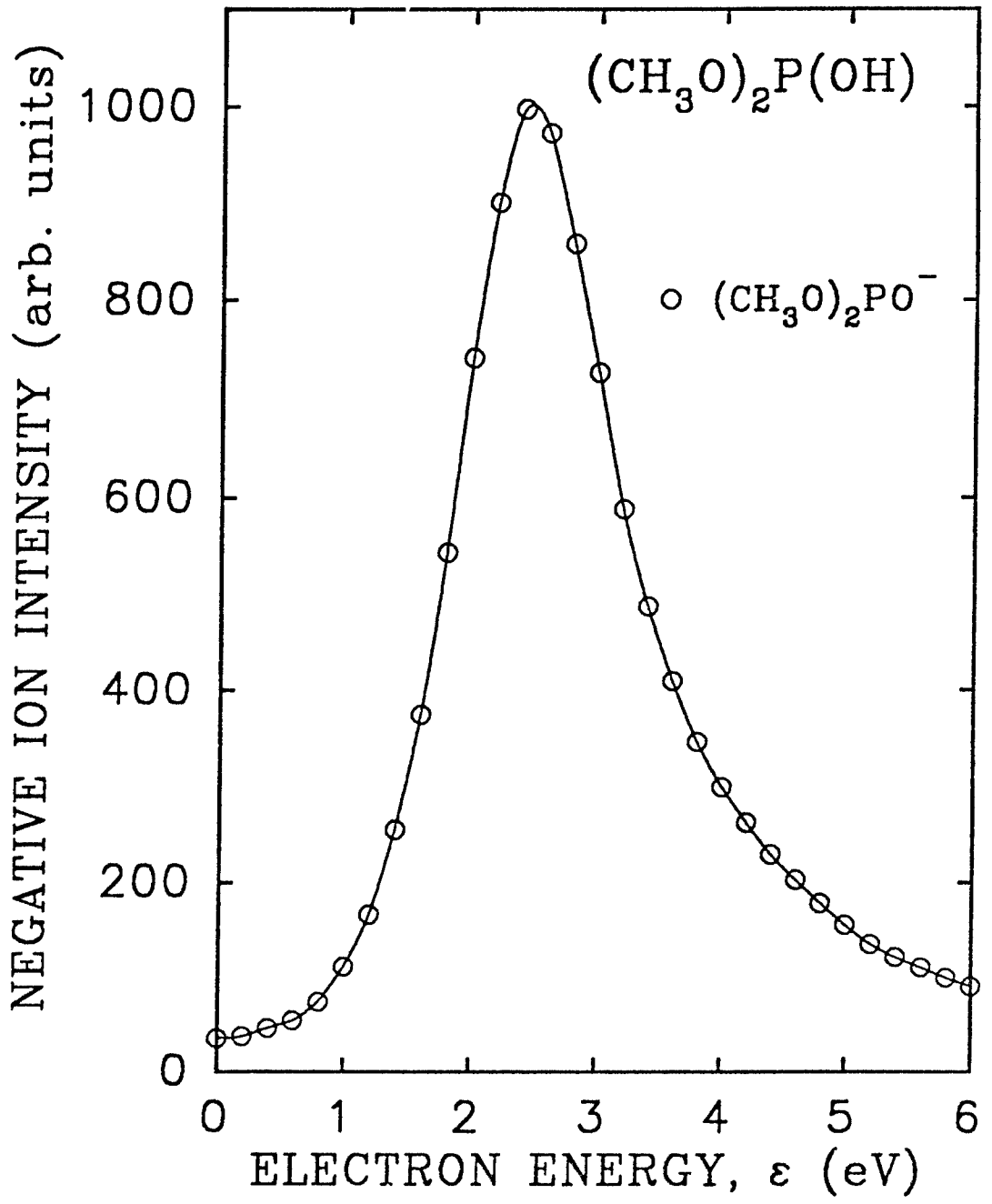

Figure 15: Negative ion intensity as a function of electron energy produced by electron impact on DMP.

Table 8: Formation of negative ions for DMP as measured in the TOF experiment

Mass (amu)	Negative Ion	Relative Intensity*	Peak Position (eV)
109	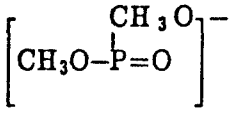	7.5×10^{-3}	2.45

*Relative intensity is 1 for SF_6^- at ~0.0 eV and at the same pressure as DMP.

3.8 Diethyl trichloro methyl phoshonate (DE3ClMP)

DE3ClMP was obtained from Pfaltz & Bauer, Inc. with a stated purity of 95%. It has a mass of ~ 254 *amu* and its chemical formula is $(C_2H_5O)_2P(O)(CCl_3)$. Its structural formula is represented by

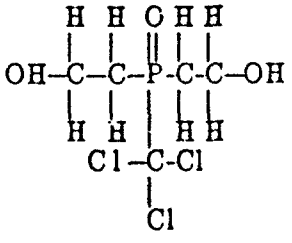

In the TOF experiment there were four negative ions observed (all below 1 eV) and only one was identified. The other three were formed due to electron attachment to impurities present in the original sample. These results are shown in Fig. 16 and are summarized in Table 9.

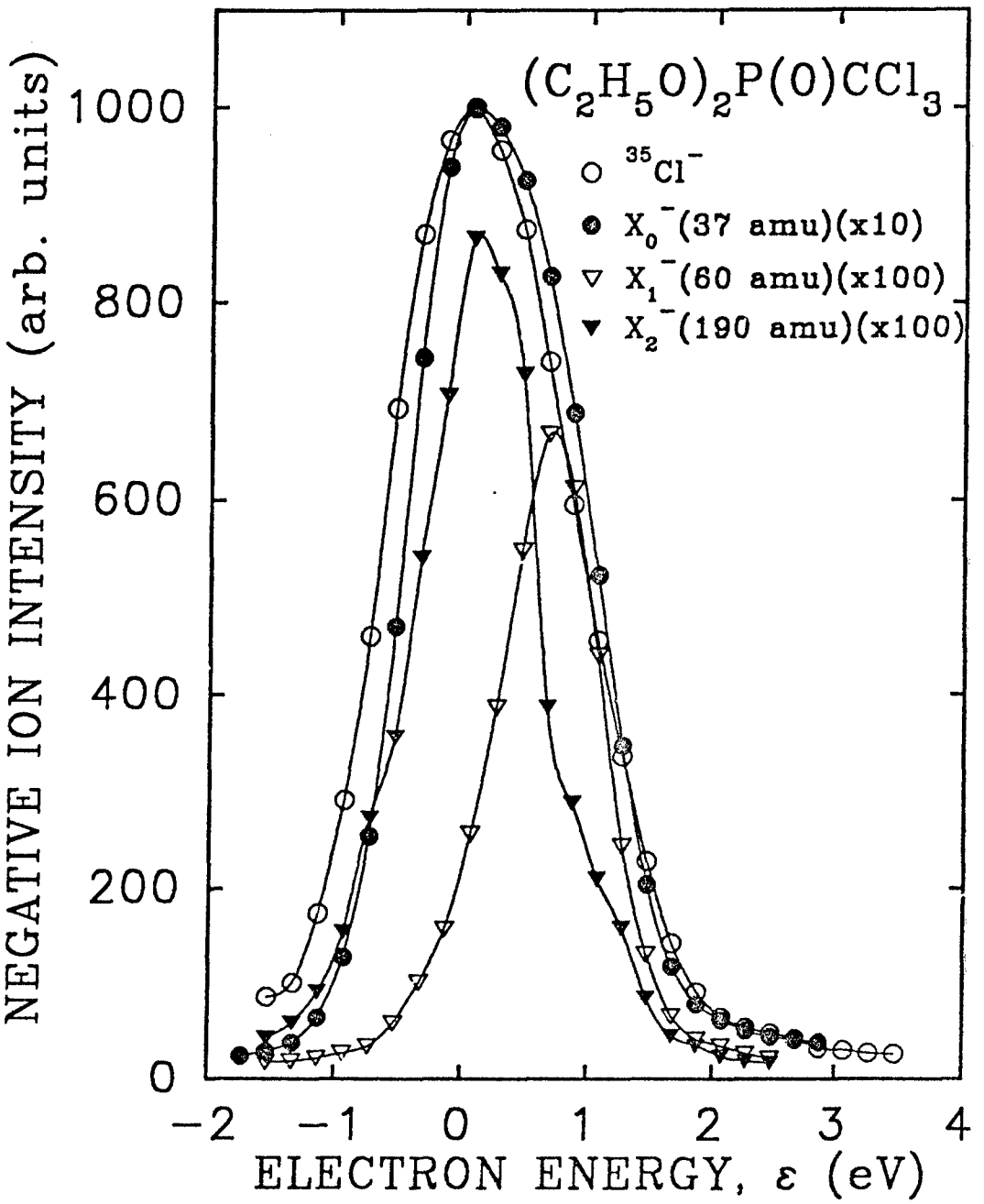

Figure 16: Negative ion intensity as a function of electron energy produced by electron impact on DE3ClMP.

Table 9: Formation of negative ions for DE3ClMP as measured in the TOF experiment

Mass (amu)	Negative Ion	Relative Intensity*	Peak Position (eV)
35	Cl^-	1.5	~0.0
37	X_0^-	0.15	~0.0
60	X_1^-	0.01	0.7
190	X_2^-	0.013	0.0

*Relative intensity is 1 for SF_6^- at ~0.0 eV and at the same pressure as DE3ClMP.

DE3ClMP was also studied by employing the PHA electron swarm technique in a buffer gas of N_2 and a pressure of ~ 1 atm and as a function of the mean electron energy $\langle\epsilon\rangle$ in the range $\sim$ 0.0 to $\sim$ 0.9 eV. The measured $k_a(\langle\epsilon\rangle)$ is plotted in Fig. 17. DE3ClMP exhibits a strong electron attachment ($k_a(\langle\epsilon\rangle) \sim 15 \times 10^{-9}$ cm^3s^{-1} at $\langle\epsilon\rangle \sim 0.0$ eV) which decreases with increasing mean electron energy. From the results from the TOF study we concluded that DE3ClMP attaches electrons purely dissociatively and that the main negative ion is Cl^-.

Negative ion mobility measurements were carried out using the PT electron swarm apparatus using ~ 4 Pa of DE3ClMP in 100 kPa of N_2. In the E/N range 3.1×10^{-18} to 3.1×10^{-17} $V\ cm^2$ (mean electron energy range of 0.04 to 0.7 eV) the negative ion mobility was constant within the experimental error and equal to 1.9 ± 0.3 $cm^2V^{-1}s^{-1}$. Addition of ~ 1.3 Pa of H_2O (water) to the mixture DE3ClMP/N_2 reduced the mobility down to ~ 1.43 $cm^2V^{-1}s^{-1}$, presumably due to cluster formation involving negative ions.

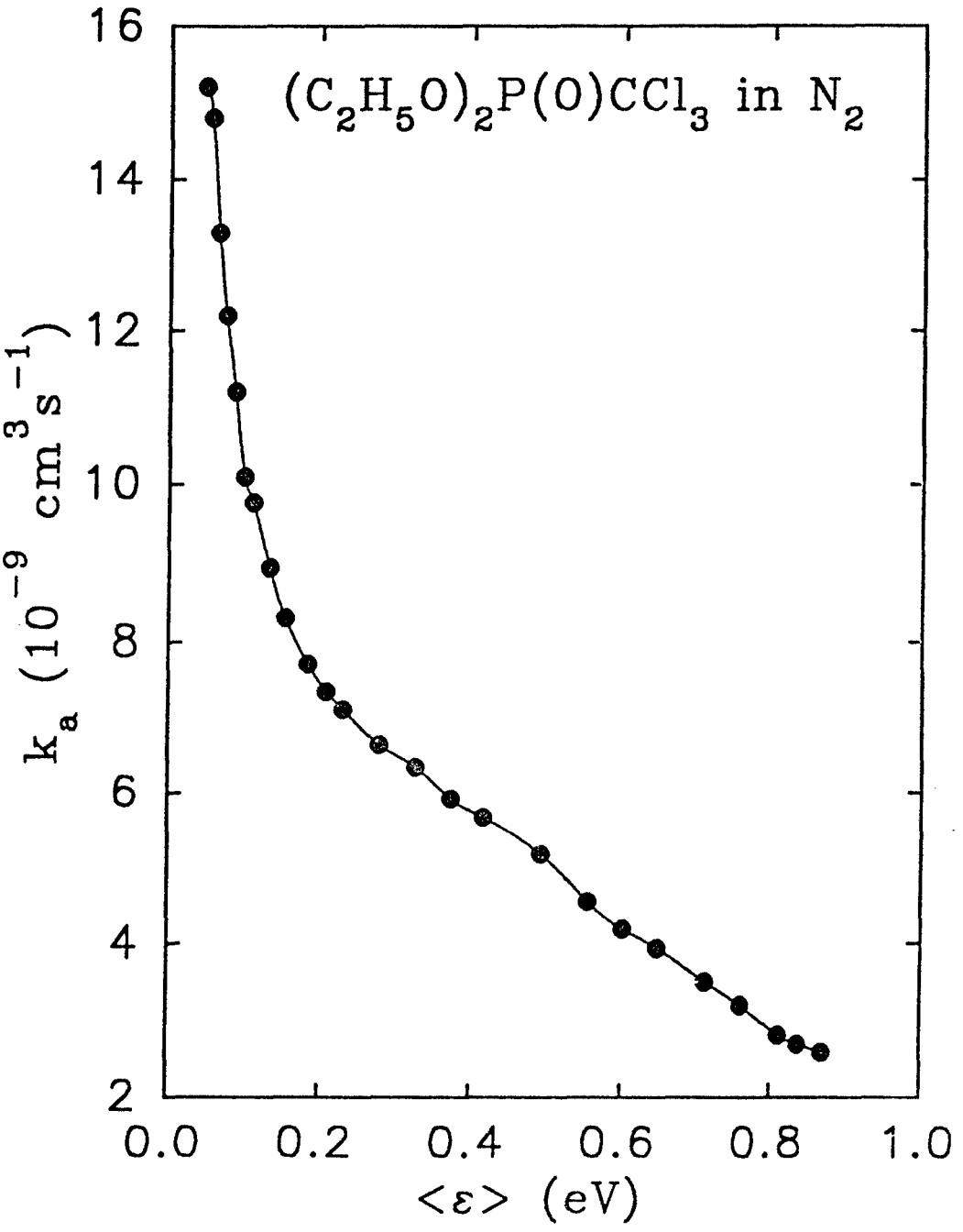

Figure 17: Electron attachment rate constant as a function of mean electron energy for DE3ClMP.

3.9 Diethyl chloro phoshate (DEClP)

DEClMP was obtained from Aldrich Chemical company with a stated purity of 97%. It has a mass of ~ 172 *amu* and its chemical formula is $(C_2H_5O)_2P(O)Cl$. Its structural formula is represented by

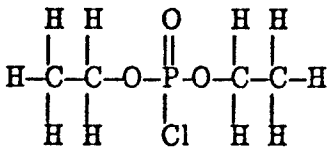

Strong negative ion formation was observed in the TOF apparatus; six different fragment anions were observed (all below 0.5 eV) and all of them except one can be tentantively identified as originating from electron attachment to the parent molecule. The observed fragmentation patterns are summarized in Table 10 along with their respective intensities (compared to the intensity of SF_6^-/SF_6). Their resonances are plotted in Fig. 18.

DEClP was also studied by employing the PHA electron swarm technique in a buffer gas of N_2 and a pressure of ~ 1 *atm* and as a function of the mean electron energy $\langle\epsilon\rangle$ in the range ~ 0.0 to ~ 0.9 eV. Consistent with the TOF measurements, strong electron attachment was observed near zero electron energy in the PHA study (see Fig. 19).

The negative ion mobility was measured and was found to be almost a constant in the E/N range of 3.0×10^{-18} to 30.0×10^{-18} Vcm^2 and equal to (1.5 ± 0.1) $cm^2V^{-1}s^{-1}$.

Even though this sample gave consistent results when it was not disturbed, it was noted that its color changed (from clear to yellow-green) when it was transfered from one electron swarm apparatus to another in order to perform the ion mobility measurements. The electron attachment rate constants were also measured and found to be an order of magnitude smaller for the discolored sample. An investigation on the effect of heat and light on DEClP revealed that it was stable up to 35 $°C$, and also was not affected by light, but it was found that it strongly reacted with the Kovar neck of the glass flask containing the sample. When the flask was turned so that the DEClP came into contact with the Kovar tubing (the transition connecting the glass to the cajon connector) a clear sample instantaneously turned green. This

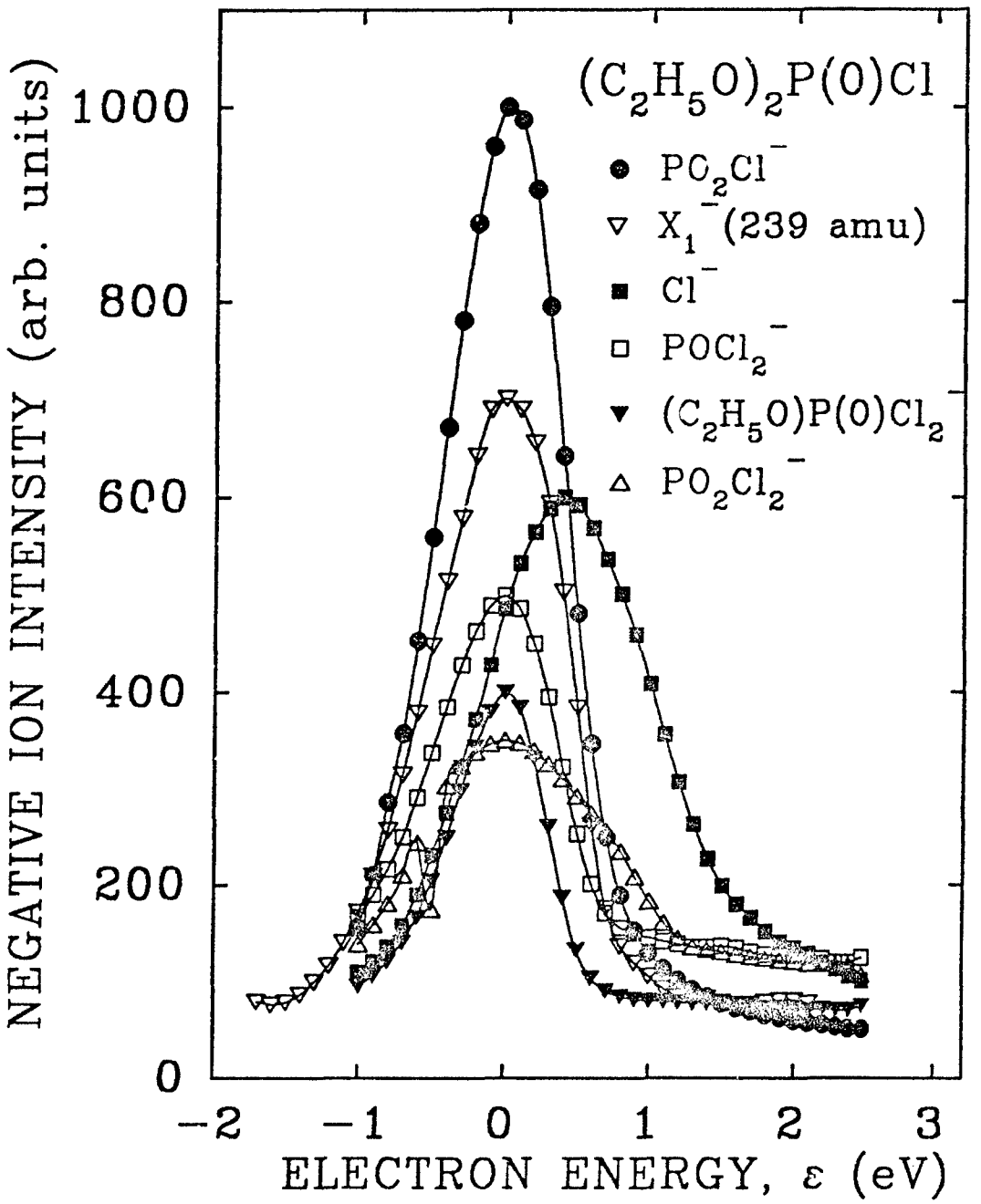

Figure 18: Negative ion intensity as a function of electron energy produced by electron impact on DEClP.

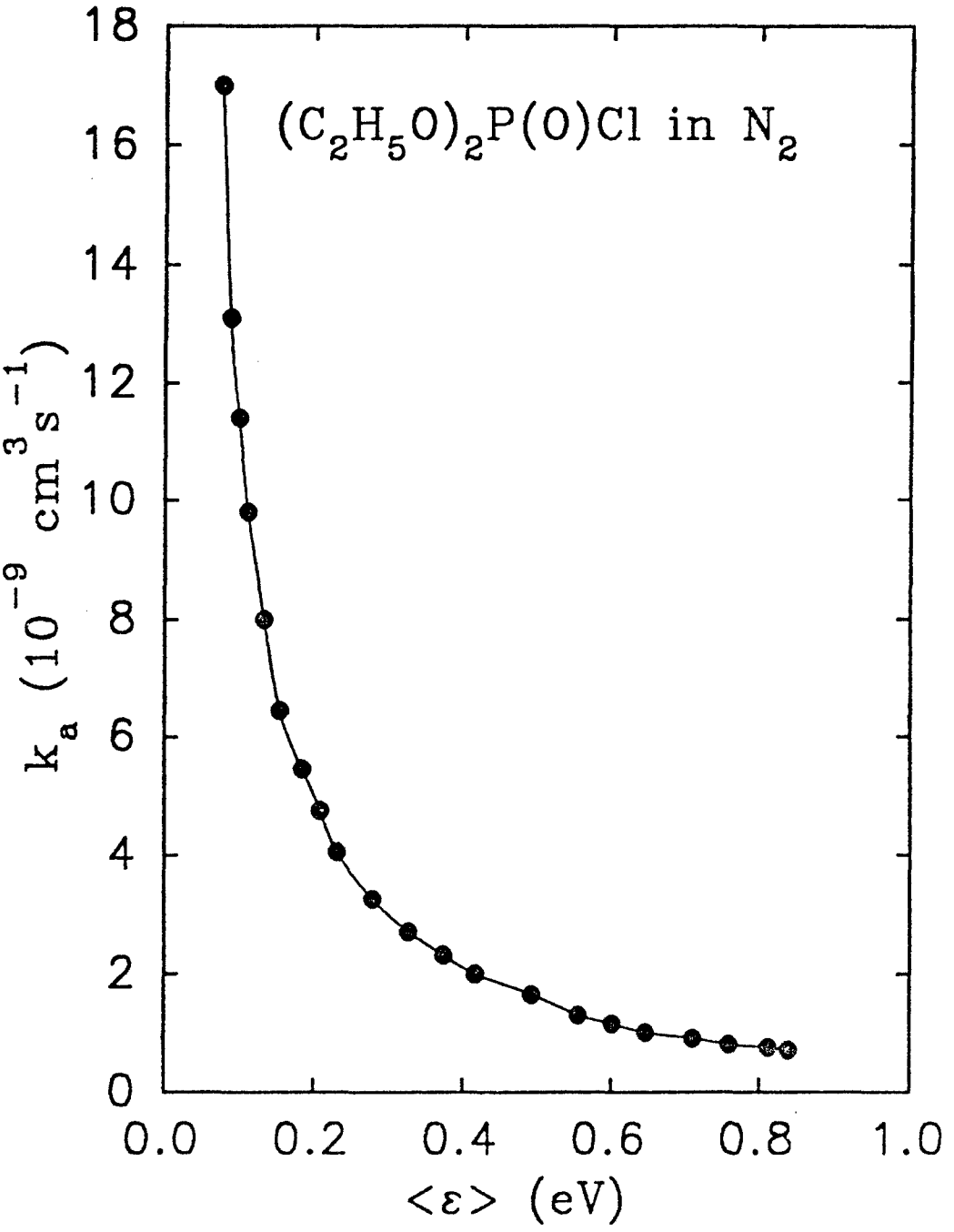

Figure 19: Electron attachment rate constant as a function of mean electron energy for DECP.

Table 10: Formation of negative ions for DEClP as measured in the TOF experiment

Mass (amu)	Negative Ion	Relative Intensity*	Peak Position (eV)
35	Cl^-	0.03	~0.4
98	PO_2Cl^-	0.06	~0.0
117	$POCl_2^-$	0.03	~0.0
133	$PO_2Cl_2^-$	0.02	~0.0
163	$(C_2H_5O)\ P(OH)\ Cl_2^-$	0.02	~0.0
239	X_1^-	0.04	~0.0

*Relative intensity is 1 for SF_6^- at ~0.0 eV and at the same pressure as DEClP.

was repeated with another flask with a longer Kovar tube and the change in color was even more profound.

In conclusion, dissociative electron attachment to DEClP was observed close to zero electron energy. Apparently the Cl^- and the PO_2Cl^- ions are the fragment negative ions initially produced; the other anions result from attachment of these two fragments anions to neutral fragments. No significant electron attachment to imputities was observed. DEClP reacts strongly with Kovar causing the sample to change color from clear to green, and this drastically reduces its electron attaching properties. DEClP is not affected by heat up to 35 $°C$.

3.10 Diethyl chloro methyl phoshonate (DEClMP)

DEClMP was obtained from Aldrich Chemical company with a stated purity of 97%. It has a mass of $\sim$ 186.58 *amu* and its chemical formula is $(C_2H_5O)_2CH_2ClP(O)$. Its structural formula is represented by

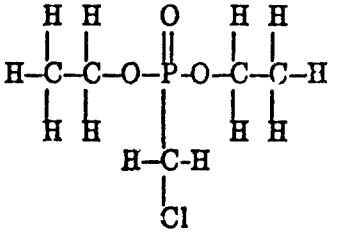

The Cl^- ions were observed in abundance around $\sim 0.8\ eV$ in the time-of-flight apparatus. This was the only anion that was observed (see Fig. 20). The anion signal due to Cl^- was $\sim$ 2% of the signal due to SF_6^- under the same conditions. The results are summarized in Table 11.

In the electron swarm study it was noticed that there is significant adsorption onto the walls of the experimental chamber (made out of stainless steel). In order to quantify this effect so that reliable electron attachment measurements could be performed, the pressure drop of DEClMP was measured as a function of the time which had elapsed from the moment the sample was introduced into the chamber; the results are shown in Fig. 21. As we see from Fig. 21 if the measurements are carried out after $\sim$ 2 to 3 hours, the error introduced by the drop in the pressure of DEClMP with time would be less than 4%. This assumes that the introduction of the buffer gas (N_2) does not alter the adsorption/desorption pattern. The measured $k_a(\langle\epsilon\rangle)$ are plotted in Fig. 22. From Fig. 22 we see that $k_a(\langle\epsilon\rangle)$ for DEClMP exhibits two peaks; one at $\langle\epsilon\rangle \sim 0.0\ eV$ and a smaller at $\langle\epsilon\rangle \sim 0.4\ eV$. The latter peak is probably due to the dissociative electron attachment to DEClMP forming Cl^-, which peaks at an electron energy of $\sim 0.8\ eV$ as shown in Fig. 22. The zero electron energy peak was not observed in the TOF study and is probably due to nondissociative electron attachment to the parent molecule.

Negative ion mobility measurements were carried out using $\sim 40\ Pa$ of DEClMP in $\sim 100\ kPa$ of N_2. In the E/N range of 9.2×10^{-19} to $3.7 \times 10^{-17}\ Vcm^2$ the negative ion mobility, μ_{ion}, was alsmost a constant and equal to $(\sim 0.27 \pm 0.10)\ cm^2V^{-1}s^{-1}$.

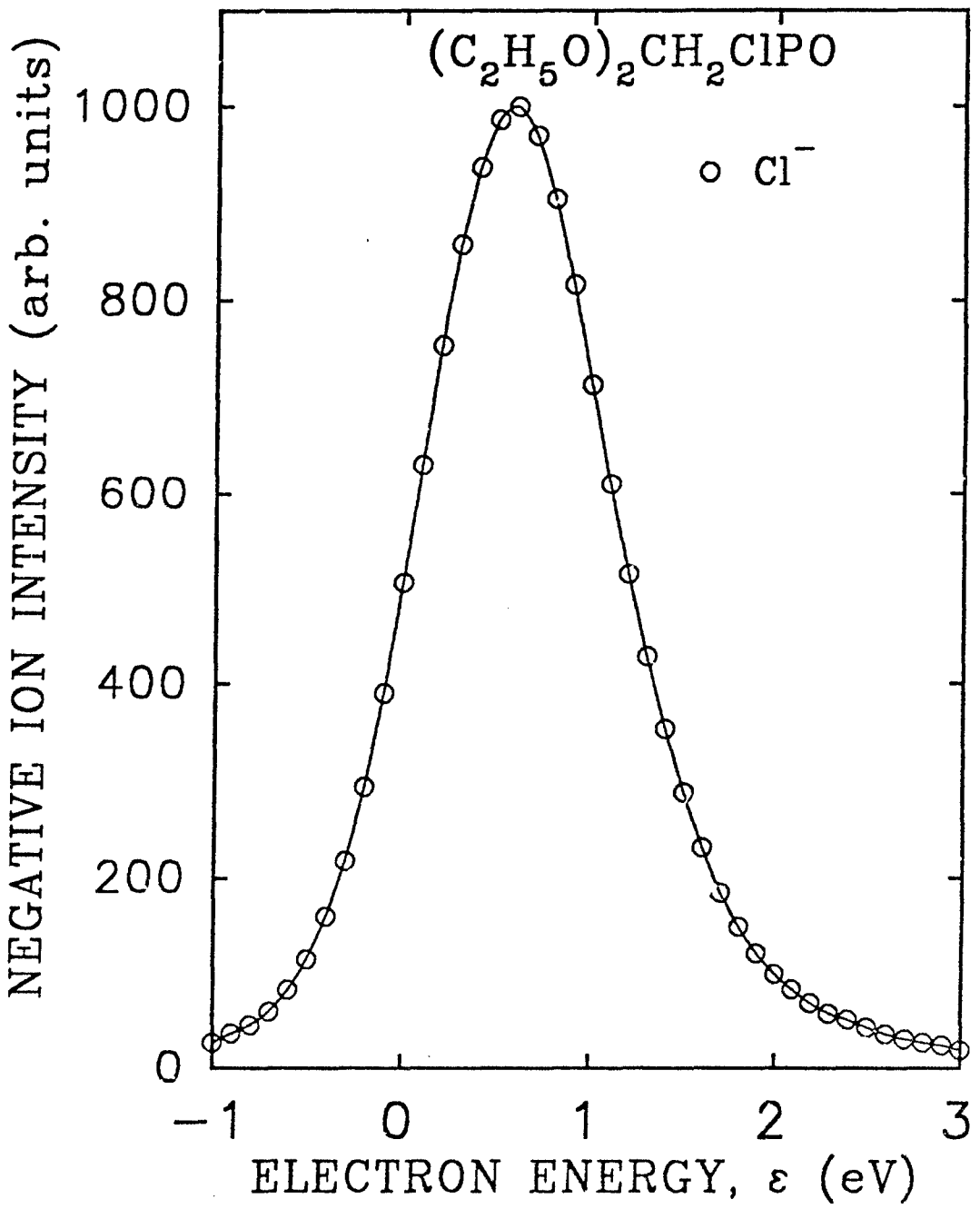

Figure 20: Negative ion intensity as a function of electron energy produced by electron impact on DECIMP.

Table 11: Formation of negative ions for DEClMP as measured in the TOF experiment

Mass (amu)	Negative Ion	Relative Intensity*	Peak Position (eV)
37	Cl^-	0.02	~0.6

*Relative intensity is 1 for SF_6^- at ~0.0 eV and at the same pressure as DEClMP.

In conclusion: (i) dissociative electron attachment produces Cl^- anions from DEClMP peaking at $\sim 0.8\ eV$, (ii) a parent anion is probably produced at $\sim 0.0\ eV$ in the high pressure electron swarm study and (iii) there is a very strong adsorption by the (stainless steel) chamber walls which introduces some uncertainty in the measured electron attachment rate constant presented in Fig. 22.

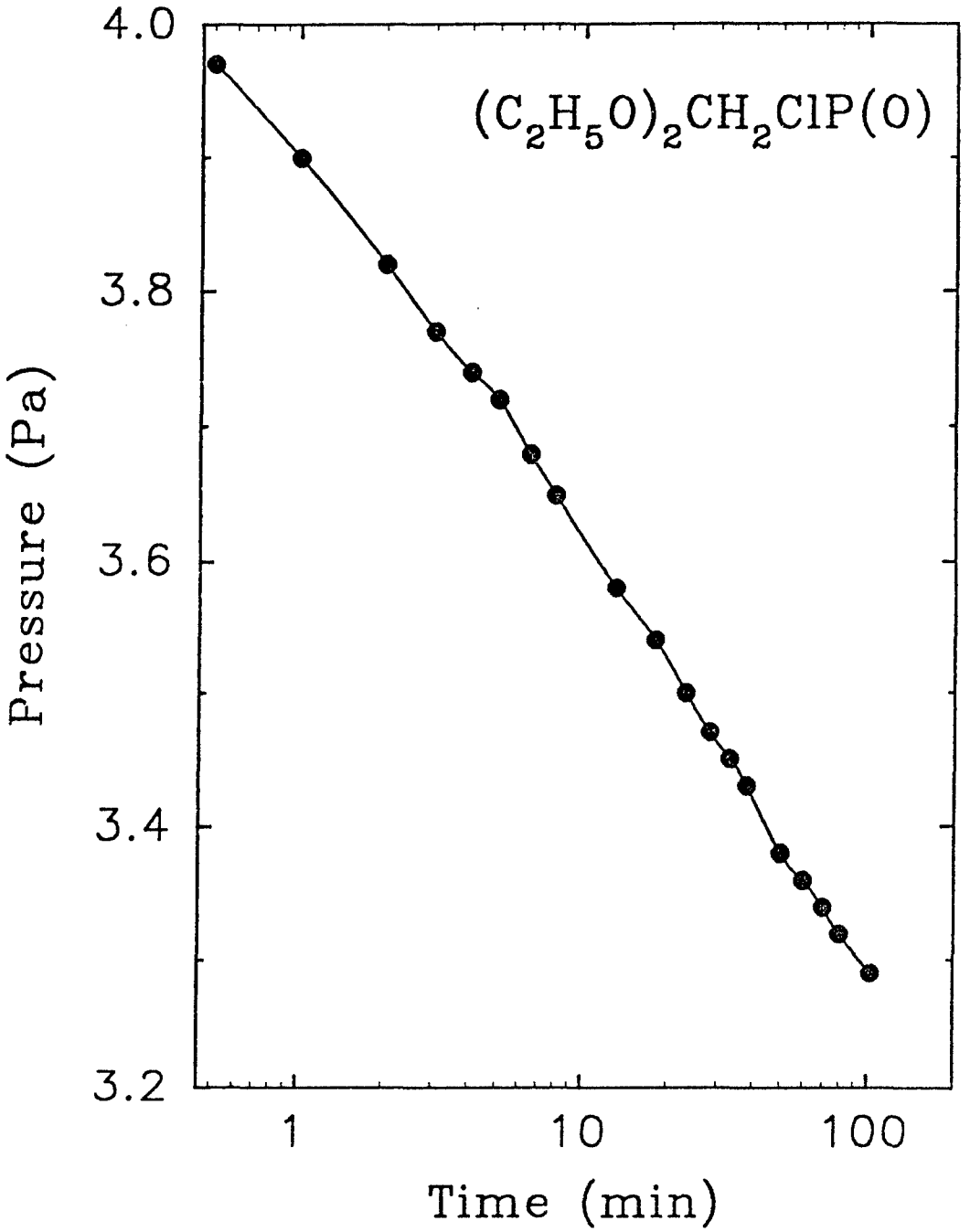

Figure 21: Pressure of DEClMP introduced into the experimental chamber as a function of time.

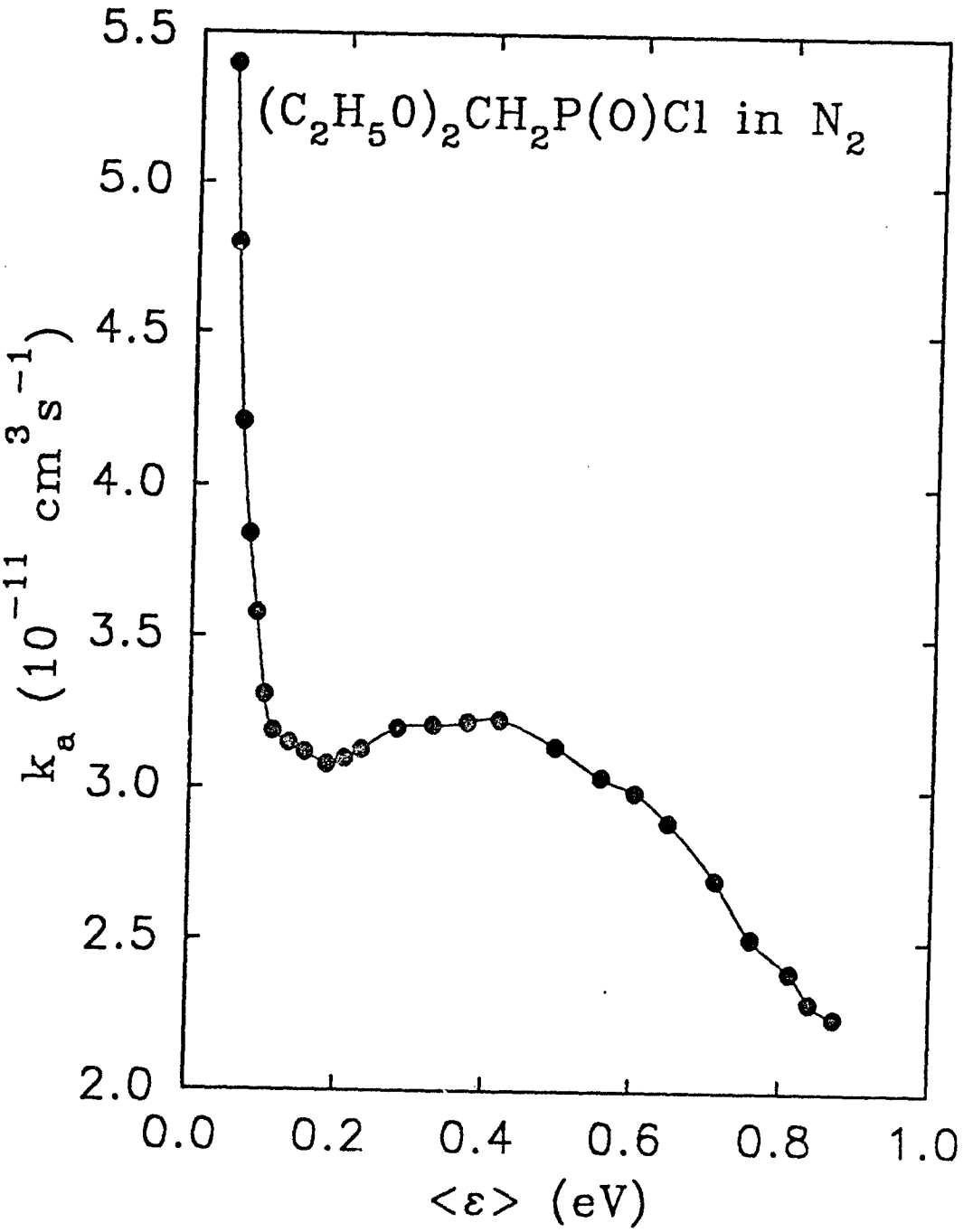

Figure 22: Electron attachment rate constant as a function of mean electron energy for DECIMP.

3.11 Diethyl cyano methyl phoshonate (DECyMP)

DECyMP was obtained from Aldrich Chemical company with a stated purity of 98%. It has a mass of ~ 177.14 *amu* and its chemical formula is $(C_2H_5O)_2CH_2(CN)P(O)$. Its structural formula is represented by

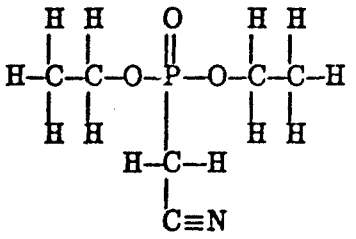

There were three negative ions observed and identified in the TOF experiment. The strongest negative ion intensity was due to dissociative electron attachment at $\epsilon \sim 0.0\ eV$ resulting in the formation of PO^-. The results are plotted in Fig. 23 and are summarized in Table 12.

DECyMP was also studied in the electron swarm experiment (PHA) in a buffer gas of N_2 at a pressure of $\sim 1\ atm$. In particular, the $k_a(\langle\epsilon\rangle)$ was measured as a function of the mean electron energy in the mean electron energy range $\langle\epsilon\rangle \sim 0.0$ to $0.9\ eV$. The results are shown in Fig. 24.

The $k_a(\langle\epsilon\rangle)$ exhibits two peaks; one at $\sim 0.0\ eV$ and another at $\sim 0.2\ eV$. The former peak can be attributed to dissociative electron attachment to DECyMP as the TOF study (Fig. 23) indicates.

Negative ion mobility measurements were carried out using $\sim 20\ Pa$ of DECyMP in $\sim 100\ kPa$ of N_2. In the E/N range of 1.5×10^{-18} to $3.7 \times 10^{-17}\ Vcm^2$ the negative ion mobility, μ_{ion}, was almost a constant and equal to $(\sim 2.0 \pm 0.1)\ cm^2V^{-1}s^{-1}$.

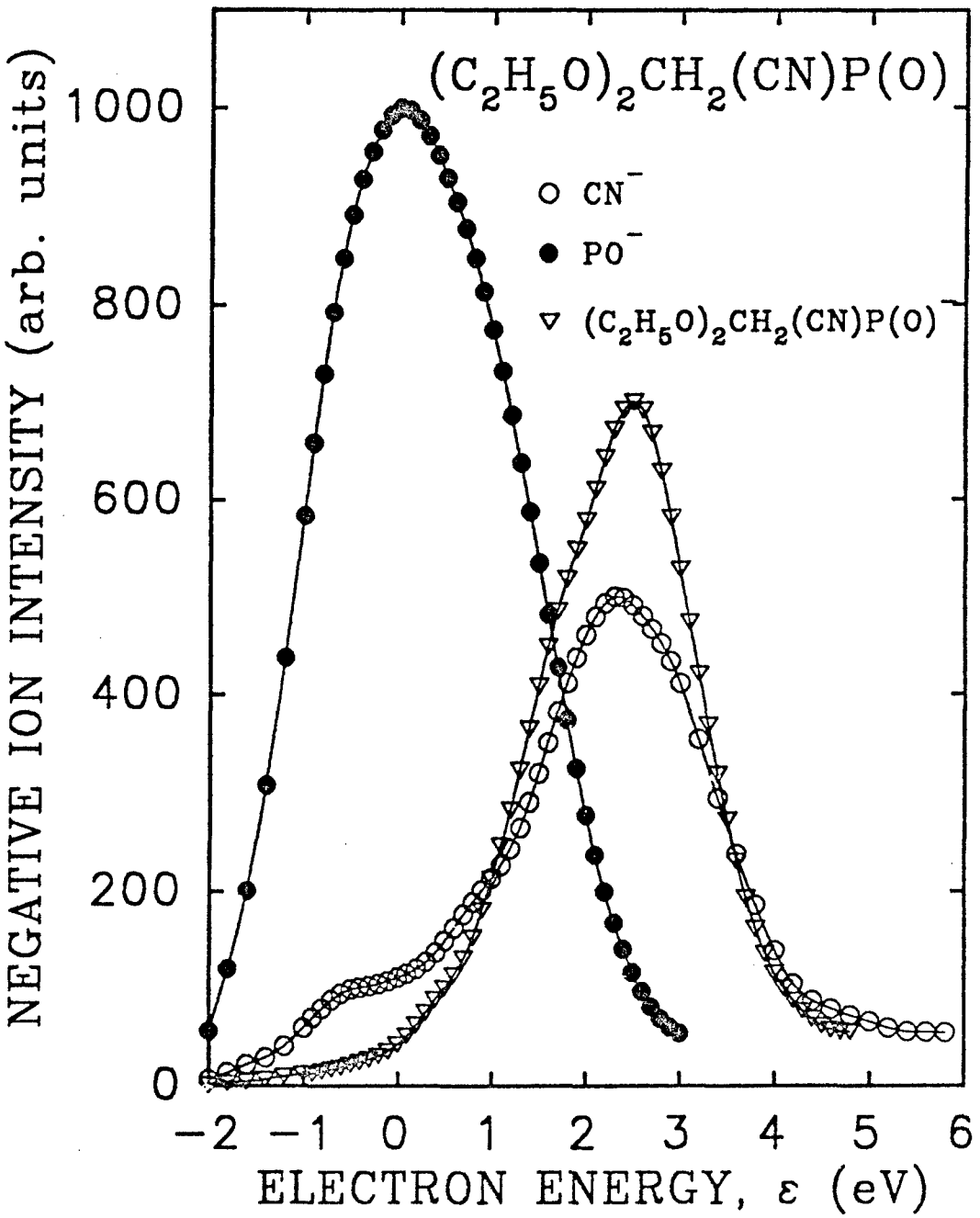

Figure 23: Negative ion intensity as a function of electron energy produced by electron impact on DECyMP.

Table 12: Formation of negative ions for DECyMP as measured in the TOF experiment

Mass (amu)	Negative Ion	Relative Intensity*	Peak Position (eV)
26	CN^-	$5x10^{-5}$	~2.4
47	PO^-	$1x10^{-4}$	~0.0
177	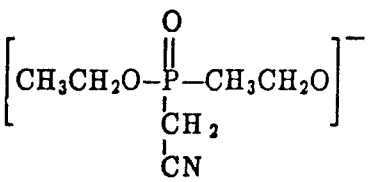	$7.x10^{-5}$	~2.5

*Relative intensity is 1 for SF_6^- at ~0.0 eV and at the same pressure as DECyMP.

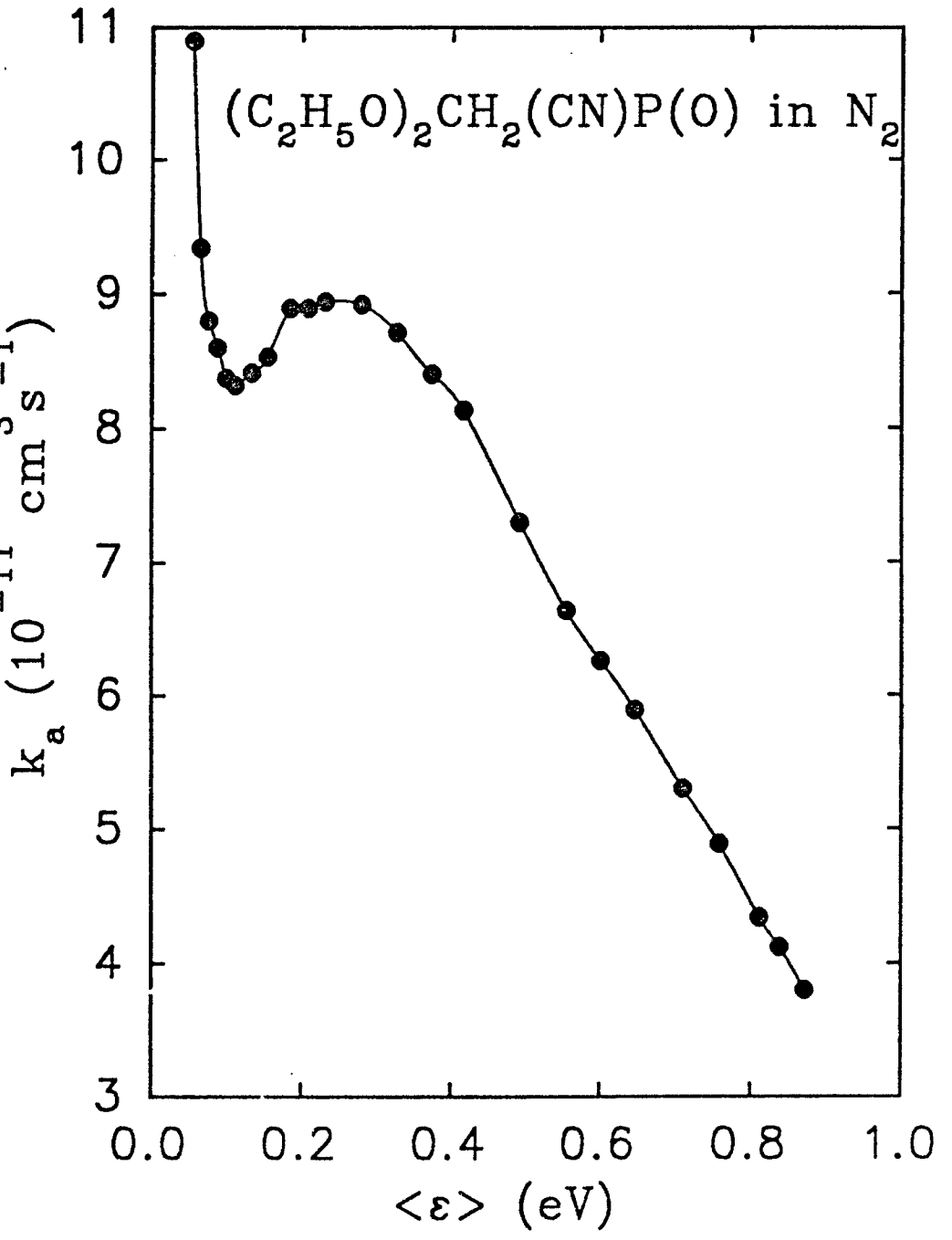

Figure 24: Electron attachment rate constant as a function of mean electron energy for DE-CyMP.

Acknowledgment

Research sponsored by Aero Propulsion and Power Directorate, Wright Laboratory, Air Force Systems Command, Wright-Patterson Air Force Base, Ohio 45433-0563 and the Office of Health and Environmental Research, U.S. Department of Energy, under contract DE-AC05-84OR21400 with Martin Marietta Energy Systems, Inc.

References

[1] S. R. Hunter and L. G. Christophorou in *Electron-Molecule Interaction and Their Applications* Ed. by L. G. Christophorou (Academic, New York 1984), Vol. 2, p. 90.

[2] L. A. Pinnaduwage, L. G. Christophorou, and S. R. Hunter, *J. Chem. Phys.* 90, 6275 (1989).

[3] T. E. Bortner and G. S. Hurst, *Phys. Rev.* 114, 116 (1958).

[4] P. G. Datskos, *Ph. D. Dissertation*, University of Tennessee, Knoxville, TN (1988).

[5] S. R. Hunter and L. G. Christophorou, *J. Chem. Phys.* 80, 6150 (1984).

[6] W. C. Wiley and I. H. McLaren, *Rev. Sci. Instr.* 26, 1150 (1955)

U.S. Government Printing Office 548-076